IMA Journal of Numerical Analysis (2025) **00**, 1–32
https://doi.org/10.1093/imanum/draf091

New Crouzeix-Raviart elements of even degree: theoretical aspects, numerical performance and applications to the Stokes' equations

A. Bressan
IMATI-CNR "E. Magenes", 27100 Pavia, Italy

L. Mascotto
Dipartimento di Matematica e Applicazioni, Università di Milano-Bicocca, 20125 Milan, Italy
IMATI-CNR "E. Magenes", 27100 Pavia, Italy
Fakultät für Mathematik, Universität Wien, 1090 Vienna, Austria

AND

M. Mosconi*
Dipartimento di Matematica e Applicazioni, Università di Milano-Bicocca, 20125 Milan, Italy
*Corresponding author: m.mosconi@campus.unimib.it

[Received on 18 February 2025; revised on 24 July 2025]

We construct new Crouzeix-Raviart (CR) spaces of even degree p in two dimensions that are spanned by basis functions mimicking those for the odd degree case. Compared to the standard CR gospel, the present construction allows for the use of nested bases of increasing degree and is particularly suited to design variable order CR methods. We analyze a nonconforming discretization of a two-dimensional Poisson problem, which requires a DG-type stabilization; the employed stabilization parameter is considerably smaller than that needed in DG methods. Numerical results are presented, which exhibit the expected convergence rates for the h-, p- and hp-versions of the scheme. We further investigate numerically the behaviour of new even degree CR-type discretizations of the Stokes' equations.

Keywords: Crouzeix-Raviart element; hierarchical basis; DG stabilization; hp-method; Stokes' equations.

1. Introduction

State-of-the-art: the finite element framework. The lowest-order Crouzeix–Raviart (CR) element was introduced in 1973 in Crouzeix & Raviart (1973) as an elementwise divergence free discretization of the Stokes' equations for space dimensions $d = 2, 3$ (see also Raviart & Thomas, 1977). Fortin & Soulie (1983) constructed explicit piecewise quadratic CR elements in 2D; they showed that the second-order CR global space is a standard conforming piecewise quadratic space enriched with elemental nonconforming bubbles. A CR scheme with cubic approximation properties in 2D was detailed in Crouzeix & Raviart (1973, Example 5) by augmenting the space with quartic bubble functions; Crouzeix & Falk (1989) later introduced an optimal CR cubic element, which did not require such bubbles. Cha *et al.* (2000) constructed quartic CR elements in 2D, where fourth order nonconforming bubbles were employed, with properties similar to those required by Fortin and Soulie in the quadratic case. In the subsequent years, the interest in developing higher (and general) order CR elements raised a lot; we refer to Stoyan & Baran (2006); Ciarlet *et al.* (2016) and Carstensen & Sauter (2022a) for (essentially up to date) developments on this topic.

In the literature, CR-type nonconforming global spaces have been defined

- *implicitly*, as spaces of piecewise polynomials satisfying certain 'no-jump' conditions at the interface between elements;
- *explicitly*, as the span of the union of standard conforming finite element functions and additional nonconforming bubble functions.

While the former version is particularly useful on the theoretical level, the latter appears to be very convenient in the implementation of the scheme.

It was clear since the very inception of the CR method Crouzeix & Raviart (1973), see also Fortin & Soulie (1983), that the *explicit* definition involves different types of basis functions depending on the order of the scheme:

- odd order CR elements are spanned by modal functions, yet removing the standard hat functions associated with the vertices of the mesh, and edge nonconforming bubbles; see Section 1.4.1;
- even degree CR elements are spanned by modal functions and elemental nonconforming bubbles; see Section 1.4.2.

Apparently, this difference leads to some limitations:

- in view of the p-version of the scheme, the corresponding basis functions have not a hierarchical structure;
- variable order CR schemes does not contain the space of piecewise affine functions, cf. Subsection 4.1.

State-of-the-art: beyond finite elements. More recent variants of CR-type elements, which on occasion (typically on triangular meshes and for low order of accuracy) coincide with CR elements, are given by the nonconforming virtual element method (Ayuso de Dios *et al.*, 2016; Brezzi & Marini, 2021; Beirão da Veiga *et al.*, 2023) and the hybrid high-order method (Di Pietro *et al.*, 2014, 2016).

Goals of the paper. In this work, we aim at facing the above issues. In particular, we design novel even degree CR spaces based on spanning sets of basis functions similar to those employed in standard CR elements with odd degree. This new approach

- gives a hierarchical structure to the resulting p-version CR method;
- allows for a simple and optimal design of variable order CR elements.

A moderate price to pay for these advantages is that the standard broken grad-grad bilinear form must be corrected with DG-type terms in order to retain error estimates of the expected order; this correction is not needed for the well-posedness of the method and, compared to its DG counterpart (Di Pietro & Ern, 2012), has a much more moderate effect on the performance of the scheme, as we shall investigate in practice.

As an interesting per se matter, we shall also check the behaviour of new even degree CR-type discretizations of the Stokes' equations on the numerical level; this aspect is very much related to the recent works (Sauter & Torres, 2023; Sauter, 2023).

Outline of the remainder of this section. After recalling some functional and finite element tools in Sections 1.1 and 1.2, we review the standard conforming modal elements in Section 1.3. Section 1.4 is devoted to the design of (implicit and explicit versions) CR elements as in Crouzeix & Raviart (1973). Eventually, the convergence analysis of standard CR methods is detailed in Section 1.5.

Outline of the paper. New CR elements (and corresponding methods) of even degree are the topic of Section 2; the theoretical results therein proven are assessed on the numerical level in Section 3; both the h- and p-versions are considered. Variable order elements are detailed in Section 4; there, we also check the performance of the hp-version of the scheme for the approximation of corner singularities. The behaviour of new even degree CR-type discretizations of the Stokes' equations is the topic of Section 5. Conclusions are drawn in Section 6.

1.1 *Functional setting and model problem*

We employ standard notation for differential operators: $\Delta\cdot$ and $\nabla\cdot$ are the Laplacian and the gradient.

Consider a bounded, Lipschitz domain Ω in $\mathbb{R}^2$ with boundary $\partial\Omega$. Let $\mathbf{n}_\Omega$ and h_Ω be its outward unit normal vector and diameter. The space $L^p(\Omega)$, p in $[1,\infty)$, is the space of Lebesgue measurable functions that are p-integrable, which we endow with the norm $\|\cdot\|_{L^p(\Omega)}$; if $p=2$, we write $\|\cdot\|_{L^2(\Omega)} = \|\cdot\|_{0,\Omega}$.

Let $\boldsymbol{\alpha}$ be a multi-index in $\mathbb{N}^2$, $|\boldsymbol{\alpha}| := \sum_{i=1}^2 \boldsymbol{\alpha}_i$ be its length, and $D^{\boldsymbol{\alpha}}$ be the distributional derivative with partial derivative of order $\boldsymbol{\alpha}_j$ along the direction x_j, $j=1,2$. For s non-negative integer and p in $[1,\infty)$, we consider the Sobolev spaces

$$W^{s,p}(\Omega) := \left\{ v \in L^p(\Omega) \,|\, D^{\boldsymbol{\alpha}} v \in L^p(\Omega) \quad \forall \boldsymbol{\alpha} \in \mathbb{N}^2,\ |\boldsymbol{\alpha}| \le s \right\}.$$

For a non-negative integer s, we denote the Sobolev space $W^{s,2}(\Omega)$ by $H^s(\Omega)$, which we endow with standard inner product $(\cdot,\cdot)_s$, seminorm $|\cdot|_{s,\Omega}$, and norm $\|\cdot\|_{s,\Omega}$; in particular, we write

$$|\cdot|_{s,\Omega}^2 := \sum_{|\boldsymbol{\alpha}|=s} \left\| D^{\boldsymbol{\alpha}} \cdot \right\|_{0,\Omega}^2, \qquad \|\cdot\|_{s,\Omega}^2 := \sum_{\ell=0}^{s} h_\Omega^{2(\ell-s)} |\cdot|_{\ell,\Omega}^2.$$

Above, for $s=0$, we are using the notation $H^0(\Omega) = L^2(\Omega)$ and $\|\cdot\|_{0,\Omega} = |\cdot|_{0,\Omega}$. For a real s, the Sobolev space $H^s(\Omega)$ is defined via Riesz-Thorin interpolation.

A trace theorem holds true for Sobolev spaces (Ern & Guermond, 2021, Theorem 3.10); in particular, there exists a continuous operator γ_Ω from $H^s(\Omega)$ in $L^2(\Omega)$ for $1/2 < s < 3/2$; we denote the image of $H^s(\Omega)$ through this operator by $H^{s-\frac{1}{2}}(\partial\Omega)$. Given g in $H^{s-\frac{1}{2}}(\partial\Omega)$, this result allows us to define the space

$$H_g^s(\Omega) := \{ v \in H^s(\Omega) \mid \gamma_\Omega(v) = g \}.$$

For $g=0$, this space coincides (Meyers & Serrin, 1964) with the closure of $C_0^\infty(\Omega)$ in $H^1(\Omega)$.

Sobolev spaces of negative order $-s$, $s>0$, are defined by duality. In particular, for $s=1$ and the $H^{-1}-H^1$ duality pairing $\langle\cdot,\cdot\rangle$, we write

$$H^{-1}(\Omega) = [H_0^1(\Omega)]', \qquad \|\cdot\|_{-1,\Omega} = \sup_{w \in H_0^1(\Omega)} \frac{\langle \cdot, w \rangle}{\|w\|_{1,\Omega}}.$$

We consider the Poisson problem

$$\begin{cases} \text{find } u \text{ such that} & \\ -\Delta u = f & \text{in } \Omega \\ u = 0 & \text{on } \partial\Omega. \end{cases} \tag{1}$$

Define the bilinear form $a : H^1(\Omega) \times H^1(\Omega) \to \mathbb{R}$ as

$$a(v, w) := (\nabla v, \nabla w)_{0,\Omega}.$$

For f in $H^{-1}(\Omega)$, a weak formulation of (1) reads

$$\begin{cases} \text{find } u \in H^1_0(\Omega) \text{ such that} & \\ a(u, v) = \langle f, v \rangle & \forall v \in H^1_0(\Omega). \end{cases} \tag{2}$$

The well-posedness of (2) is standard and follows from Lax-Milgram's lemma.

1.2 *Meshes, and broken Sobolev and polynomial spaces*

We consider sequences $\{\mathcal{T}_h\}$ of conforming simplicial meshes in two dimensions, and corresponding sequences of edges $\{\mathcal{F}_h\}$ (resp. vertices $\{\mathcal{V}_h\}$), which we further split into boundary $\{\mathcal{F}_h^B\}$ (resp. $\{\mathcal{V}_h^B\}$) and internal $\{\mathcal{F}_h^I\}$ (resp. $\{\mathcal{V}_h^I\}$) edges (resp. vertices). For a given element K in a mesh $\mathcal{T}_h$, $\mathbf{n}_K$ and h_K denote its unit outward normal vector and diameter; we denote the maximum diameter of a mesh $\mathcal{T}_h$ by $h := \max_{K\in\mathcal{T}_h} h_K$. For a given edge F in $\mathcal{F}_h$, $\mathbf{n}_F$ and h_F denote a fixed once-and-for-all unit normal vector and its length; on boundary edges, we fix $\mathbf{n}_F = \mathbf{n}_{K|F}$. The sets of edges and vertices of a given element K are $\mathcal{F}^K$ and $\mathcal{V}^K$, respectively. The vertices of K are denoted by $v_{i,K}$, $i = 1, 2, 3$, and the corresponding barycentric coordinates by $\lambda_{K,i}$; when convenient, we shall replace $\lambda_{K,i}$ with $\lambda_{K,F}$ where F is the edge opposite to the ith vertex, and, when no confusion occurs, we shall omit the subscript K[1]. For F in $\mathcal{F}_h$, we define edge patches

$$\omega_F := \bigcup \left\{ K \in \mathcal{T}_h \mid F \in \mathcal{F}^K \right\}. \tag{3}$$

We demand some regularity on the sequences of meshes: the ratio between the maximum inradius and the minimum exradius of all the elements in each mesh of the sequence is uniformly bounded; in particular, there exists ρ larger than or equal to 1 such that

$$h_K \le \rho\, h_F \qquad \forall F \in \mathcal{F}^K,\ K \in \mathcal{T}_h,\ \mathcal{T}_h \in \{\mathcal{T}_h\}. \tag{4}$$

With each mesh and non-negative s, we associate the broken Sobolev spaces

$$H^s(\mathcal{T}_h, \Omega) := \{v \in L^2(\Omega) \mid v_{|K} \in H^s(K) \quad \forall K \in \mathcal{T}_h\};$$

[1] Here, the barycentric coordinate associated with the ith vertex or the opposite edge F is the linear Lagrangian function equal to 1 at that vertex and zero on F.

we further associate the broken gradient $\nabla_h : H^1(\mathcal{T}_h, \Omega) \to [L^2(\Omega)]^2$ defined as $(\nabla_h v)_{|K} := \nabla(v_{|K})$, and the broken seminorm and norm

$$|v|^2_{1,h;\Omega} := (\nabla_h v, \nabla_h v)_{0,\Omega}, \qquad \|v\|^2_{1,h;\Omega} := h_\Omega^{-2}\|v\|^2_{0,\Omega} + |v|^2_{1,h;\Omega}. \tag{5}$$

For each edge F in $\mathcal{F}_h$ and v in $H^{\frac{1}{2}+\varepsilon}(\mathcal{T}_h)$, ε positive, we introduce the jump

$$[\![v]\!]_F = [\![v]\!] := \begin{cases} \gamma_{K_1}(v)_{|F}(\mathbf{n}_{K_1} \cdot \mathbf{n}_F) + \gamma_{K_2}(v)_{|F}(\mathbf{n}_{K_2} \cdot \mathbf{n}_F) & F \in \mathcal{F}_h^I,\ F = \partial K_1 \cap \partial K_2 \\ \gamma_K(v)_{|F} & F \in \mathcal{F}_h^B,\ F = \partial\Omega \cap \partial K \end{cases} \tag{6}$$

and average operators (taking values in $L^2(F)$)

$$\{v\}_F = \{v\} = \begin{cases} \frac{1}{2}(\gamma_{K_1}(v) + \gamma_{K_2}(v))_{|F} & F \in \mathcal{F}_h^I,\ F = \partial K_1 \cap \partial K_2 \\ \gamma_K(v)_{|F} & F \in \mathcal{F}_h^B,\ F = \partial\Omega \cap \partial K. \end{cases}$$

The vector version of these operators is defined analogously and the operator symbols are the same.

We denote the space of polynomials of order smaller than or equal to a non-negative integer p over an element K or an edge F by $\mathbb{P}_p(K)$ and $\mathbb{P}_p(F)$. If p is a negative integer, then these two spaces are set to $\{0\}$. We further define

$$\mathbb{P}_p(\mathcal{T}_h) := \left\{ q_p \in L^2(\Omega) \middle| q_{p|K} \in \mathbb{P}_p(K) \quad \forall K \in \mathcal{T}_h \right\}$$

and

$$\mathbb{P}_p^B(\mathcal{T}_h) := \left\{ q_p \in L^2(\partial\Omega) \middle| q_{p|F} \in \mathbb{P}_p(F) \quad \forall F \in \mathcal{F}_h^B \right\}.$$

We are now in a position to define nonconforming Sobolev spaces of degree p and order s larger than $1/2$:

$$H_p^{s,nc}(\mathcal{T}_h, \Omega) := \left\{ v \in H^s(\mathcal{T}_h, \Omega) \middle| ([\![v]\!]_F, q_{p-1}^F)_{0,F} = 0 \quad \forall q_{p-1}^F \in \mathbb{P}_{p-1}(F),\ \forall F \in \mathcal{F}_h^I \right\}. \tag{7}$$

We can include 'boundary conditions' in the nonconforming space above in a weak sense: given g in $L^1(F)$ for all boundary edges F, we set

$$H_{p,g}^{s,nc}(\mathcal{T}_h, \Omega) := \left\{ v \in H_p^{s,nc}(\mathcal{T}_h, \Omega) \middle| ([\![v]\!]_F, q_{p-1}^F)_{0,F} = (g, q_{p-1}^F)_{0,F} \quad \forall q_{p-1}^F \in \mathbb{P}_{p-1}(F),\ \forall F \in \mathcal{F}_h^B \right\}. \tag{8}$$

For positive a and b, we shall denote with $a \lesssim b$ the existence of a positive constant C only depending on the domain Ω, the constant ρ in (4), and on occasions on the polynomial degree, such that $a \leq C\, b$.

A generalized Poincaré–Friedrichs inequality holds true Brenner (2003):

$$\|v\|_{0,\Omega} \lesssim |v|_{1,h;\Omega} \qquad \forall v \in H^{1,nc}_{1,0}(\mathcal{T}_h, \Omega). \tag{9}$$

As a matter of notation, given $\alpha, \beta > -1$, $L_p(\cdot)$ and $J_p^{(\alpha,\beta)}(\cdot)$ denote the univariate Legendre and Jacobi polynomials of degree p over $\widehat{I} := [-1, 1]$.

1.3 *Conforming (modal) finite elements*

We introduce the standard conforming finite element space of order p

$$X_n := \{v_n \in H^1(\Omega) \mid v_{n|K} \in \mathbb{P}_p(K) \quad \forall K \in \mathcal{T}_h\}. \tag{10}$$

An explicit basis of this space is detailed in Szabó & Babuška (1991). Here, we recall the basis functions on the reference element $\widehat{K}$ with vertices $(-1,0)$, $(1,0)$ and $(0,\sqrt{3})$, and, with an abuse of notation, barycentric coordinates $\widehat{\lambda}_{\widehat{K},\widehat{F}_i}$, $\widehat{F}_i$ in $\mathcal{F}^{\widehat{K}}$ for $i = 1,2,3$. On $\widehat{K}$, we distinguish three different types of basis functions:

- given $\widehat{v}_m$, $m = 1,2,3$, the vertices of $\widehat{K}$, the hat functions

$$\widehat{\varphi}^{\widehat{v}_1} = \frac{1}{2}\left(1 - x - \frac{y}{\sqrt{3}}\right), \qquad \widehat{\varphi}^{\widehat{v}_2} = \frac{1}{2}\left(1 + x - \frac{y}{\sqrt{3}}\right), \qquad \widehat{\varphi}^{\widehat{v}_3} = \frac{y}{\sqrt{3}};$$

- given the edges $\widehat{F}_i$, $i = 1,2,3$, of $\widehat{K}$, the $\dim(\mathbb{P}_{p-2}(\widehat{F}))$ edge bubble functions

$$\widehat{\varphi}_j^{\widehat{F}_i} := \frac{8\sqrt{4j+2}}{j(j+1)}\widehat{\lambda}_{\widehat{F}_{i \bmod 3+1}}\widehat{\lambda}_{\widehat{F}_{(i+1) \bmod 3+1}} L_j'\left(-\widehat{\lambda}_{\widehat{F}_{i \bmod 3+1}} + \widehat{\lambda}_{\widehat{F}_{(i+1) \bmod 3+1}}\right)$$
$$\forall i = 1,2,3,\ j = 1,\ldots,p-1; \tag{11}$$

- given the natural bijection between ℓ in $\{1,\ldots,\dim \mathbb{P}_{p-3}(\widehat{K})\}$ and (r_1,r_2) in $\{0,\ldots,p-3\}^2$ with $r_1 + r_2 \le p-3$, the $\dim(\mathbb{P}_{p-3}(\widehat{K}))$ elemental bubble functions

$$\widehat{\varphi}_\ell^{\widehat{K}} = \widehat{\varphi}_{r_1,r_2}^{\widehat{K}} := \widehat{\lambda}_{\widehat{F}_1}\widehat{\lambda}_{\widehat{F}_2}\widehat{\lambda}_{\widehat{F}_3} L_{r_1}(\widehat{\lambda}_{\widehat{F}_2} - \widehat{\lambda}_{\widehat{F}_1}) L_{r_2}(2\widehat{\lambda}_{\widehat{F}_3} - 1)$$
$$\forall r_1, r_2 \text{ with } r_1 + r_2 = 0,\ldots,p-3. \tag{12}$$

1.4 *Arbitrary order, standard Crouzeix-Raviart elements in 2D*

We introduce the Crouzeix-Raviart (CR) space (Crouzeix & Raviart, 1973; Raviart & Thomas, 1977) of positive integer order p:

$$V_n^{\mathrm{im}} := \{v_n \in H_p^{1,nc}(\mathcal{T}_h,\Omega) \mid v_{n|K} \in \mathbb{P}_p(K) \quad \forall K \in \mathcal{T}_h\}. \tag{13}$$

In two dimensions, this spaces coincides (Ainsworth & Rankin, 2008) with the following space:

$$V_n^{\mathrm{im}} = \{v_n \in \mathbb{P}_p(\mathcal{T}_h) \mid v_n \text{ is continuous at the Gauß–Legendre nodes of order } p \text{ on each } F \in \mathcal{F}_h^I\}.$$

We shall refer to these spaces, which are nonconforming in the sense of Strang (1972), as the *implicit* CR spaces of order p. It is known (Baran & Stoyan, 2007) that unisolvent sets of degrees of freedom for the space V_n^{im} are different for odd and even p.

An alternative way (Stoyan & Baran, 2006; Baran & Stoyan, 2007) to construct nonconforming spaces *á la* Crouzeix-Raviart consists in defining *explicit* spaces, i.e., spans of H^1 conforming finite element functions *plus* extra nonconforming bubbles. In Sections 1.4.1 and 1.4.2 below, we provide details on such bubble functions in two dimensions for odd and even degrees, respectively; show that the *implicit* and *explicit* constructions deliver exactly the same spaces; exhibit unisolvent sets of degrees of freedom.

1.4.1 *Standard Crouzeix-Raviart elements (odd degree).* Let p be an odd positive integer. Given K an element, consider for all F in $\mathcal{F}^K$ the mapped Legendre polynomials L_j^F on F, j non-negative integer, and a basis $\{m_{\boldsymbol{\beta}}^K\}_{|\boldsymbol{\beta}|=0}^{p-3}$ of $\mathbb{P}_{p-3}(K)$ consisting of elements that are invariant with respect to dilations and translations. We introduce a set of linear functionals: given v in $W^{1,1}(K)$, which admits trace in $L^1(F)$ for all F in $\mathcal{F}^K$ (Ern & Guermond, 2021, Theorem 3.10)[2],

$$|F|^{-1}\left(v, L_j^F\right)_{0,F} \qquad \forall j = 0, \ldots, p-1, \quad \forall F \in \mathcal{F}^K; \tag{14a}$$

$$|K|^{-1}\left(v, m_{\boldsymbol{\beta}}^K\right)_{0,K} \qquad \forall |\boldsymbol{\beta}| = 0, \ldots, p-3. \tag{14b}$$

A crucial property of the above linear functionals is detailed in the next result.

Lemma 1.1. Given K in $\mathcal{T}_h$ and an odd p, the linear functionals (14) are a unisolvent set of degrees of freedom for $\mathbb{P}_p(K)$.

Proof. Let v_n be in $\mathbb{P}_p(K)$ such that the moments (14) are zero. The number of linear functionals in (14) is equal to $\dim(\mathbb{P}_p(K))$; therefore, it suffices to prove that v_n is identically zero over K.

Given an edge F in $\mathcal{F}^K$, using that the edge moments (14a) are zero, the restriction of v_n on F belongs to $\mathbb{P}_p(F)$ and is orthogonal to $\mathbb{P}_{p-1}(F)$. Hence, there exists c in $\mathbb{R}$ such that $v_{n|F}(\xi) = c\, L_p^F(\xi)$ for all F in $\mathcal{F}^K$. Recall (Shen *et al.*, 2011, eq. (3.175)) that $L_p(-1) = (-1)^p = -1$ and $L_p(1) = 1$. Since p is odd and $v_{n|\partial K}$ belongs to $\mathcal{C}^0(\partial K)$, the following identities are valid:

$$v_n(v_1) = -v_n(v_2) = v_n(v_3) = -v_n(v_1). \tag{15}$$

Therefore, $v_n(v_1) = v_n(v_2) = v_n(v_3) = 0$ and there exists q_{p-3}^K in $\mathbb{P}_{p-3}(K)$ such that $v_n = \lambda_1\lambda_2\lambda_3 q_{p-3}^K$. Using that the elemental moments (14b) are zero as well, we infer $(\lambda_1\lambda_2\lambda_3(q_{p-3}^K), q_{p-3}^K)_{0,K} = 0$. Since the product of the barycentric coordinates in K is positive, we deduce that q_{p-3}^K vanishes in K. □

Remark 1. An alternative avenue to define edges degrees of freedom consists in replacing (14a) by point evaluations at the p Gauß-Legendre nodes (Raviart & Thomas, 1977, Lemma 5); from an historic point of view, this was the original approach in Crouzeix & Raviart (1973).

[2] The integrals in (14) have to be understood as duality pairings in $L^1 - L^\infty$. Similar comments will be omitted in the sequel.

Next, we discuss an alternative definition for CR elements of odd degree. With each edge F in $\mathcal{F}_h$, we associate the edge nonconforming bubble function Stoyan & Baran (2006)

$$b_p^F := \begin{cases} L_p\left(1 - 2\lambda_{K,F}\right) & \forall K \in \mathcal{T}_h,\ K \subset \omega_F \\ 0 & \text{otherwise.} \end{cases} \tag{16}$$

Under the notation in Section 1.3, we define

$$V_n^{\text{ex}} := \text{span}\left(b_p^F \text{ and } \{\varphi_j^F\}_{j=1}^{p-1} \quad \forall F \subset \mathcal{F}_h; \quad \{\varphi_\ell^K\}_{\ell=1}^{(p-1)(p-2)/2} \quad \forall K \in \mathcal{T}_h\right). \tag{17}$$

The bubble function b_p^F does not belong to X_n in (10), whence the name *nonconforming*. As discussed in Stoyan & Baran (2006); Ciarlet *et al.* (2016) and Carstensen & Sauter (2022b), the functions spanning the right-hand side of (17) are linearly independent. This fact allows us to define an explicit basis for V_n^{ex}; the corresponding degrees of freedom are the coefficients of the expansion with respect to that basis.

The next result investigates the relation between the spaces V_n^{im} and V_n^{ex} for odd p.

LEMMA 1.2. The spaces V_n^{im} and V_n^{ex} defined in (13) and (23) coincide for odd p.

Proof. Let N_F^T, N_F^I, and N_K denote the number of total edges, internal edges, and elements of $\mathcal{T}_h$, respectively. We split the proof in two steps.

V_n^{ex} is contained in V_n^{im}. The space V_n^{ex} consists of modal basis functions, i.e., functions that are H^1 conforming and therefore contained in V_n^{im}, and edge bubble functions as in (16). Such bubble functions have vanishing jumps of order up to $p-1$ over all the edges in $\mathcal{F}_h$.

To see this, we fix a generic F in $\mathcal{F}_h$ and b_p^F as in (16). We have that b_p^F is continuous over the interior of ω_F, whence it has vanishing jumps over F. On the edges $\widetilde{F}$ lying on $\partial\omega_F$, $b_{p|\widetilde{F}}^F$ is the univariate Legendre polynomial of order p starting from the vertex opposite to F; in particular, its moments with univariate polynomials of order $p-1$ are zero over $\widetilde{F}$. On the other edges of the mesh, the bubble is zero by definition, whence it has zero jumps.

V_n^{im} and V_n^{ex} have the same dimension. The dimension of V_n^{im} is the dimension of piecewise polynomials of maximum order p over $\mathcal{T}_h$, minus the total number of "no jump" conditions over the internal edges:

$$\dim(V_n^{\text{im}}) = \dim(\mathbb{P}_p(\mathcal{T}_h)) - pN_F^I = \dim(\mathbb{P}_p(K))N_K - pN_F^I. \tag{18}$$

On the other hand, the dimension of V_n^{ex} is given by the number of total edges (for the nonconforming bubbles) plus the number of modal basis functions excluding those associated with the vertices:

$$\dim(V_n^{\text{ex}}) = N_F^T + \dim(\mathbb{P}_{p-2}(F))N_F^T + \dim(\mathbb{P}_{p-3}(K))N_K = pN_F^T + \dim(\mathbb{P}_{p-3}(K))N_K. \tag{19}$$

Recall the Euler's formula

$$N_F^I + N_F^T = 3N_K. \tag{20}$$

Subtracting the identities in (18) and (19), we deduce

$$\frac{(p+2)(p+1)-(p-1)(p-2)}{2}N_K - p(N_F^I + N_F^T) \overset{(20)}{=} 0.$$

□

Lemma 1.2 entails that two different sets of degrees of freedom are at disposal. A set of global degrees of freedom for Crouzeix-Raviart spaces is obtained by a coupling of the degrees of freedom in (14a); alternatively, we pick the coefficients in the expansion with respect to the basis in (17). The former is used on the theoretical level, e.g., while deriving interpolation estimates in CR spaces, see Remark 4 below; the latter is typically used in the practice for the implementation of the method.

REMARK 2. Throughout, we shall be proving results similar to Lemma 1.3. Another reason why we distinguish the implicit and explicit spaces is that in higher dimension the two definitions do not coincide in general; cf., e.g., Sauter & Torres (2023).

1.4.2 *Standard Crouzeix-Raviart elements with even degree.* Proceeding as in Section 1.4.1 for even p, we are not able to show unisolvence of the degrees of freedom (14): the proof of Lemma 1.1 fails since display (15) would read

$$v_n(v_1) = v_n(v_2) = v_n(v_3) = v_n(v_1), \tag{21}$$

which does not imply that v_n is zero at the vertices of K; furthermore, using Gauß-Legendre-type degrees of freedom as those discussed in Remark 1 would lead to a linear dependence condition as described in Fortin & Soulie (1983, pp. 506–507) for the case $p = 2$.

We recall some details here; the general even degree case presents similar limitations. Given a triangle K, we denote its unit tangential vector and the corresponding tangential derivative by $\boldsymbol{\tau}_K$ and $\partial_{\boldsymbol{\tau}_K}$. Let $\{g_j^i\}_{i=1}^2$ and m_j denote the Gauß–Legendre quadrature points and the midpoints of the edge $F_j, j = 1, 2, 3$, respectively.

Given a quadratic polynomial q_2, $\partial_{\boldsymbol{\tau}_K} q_{2|\partial K}$ is piecewise linear: the integral over the edge F_j of $\partial_{\boldsymbol{\tau}_K} q_2$ is equal to the evaluation at the midpoint m_j; in turn, this can be expressed as the difference of the evaluation at the two Gauß-Legendre nodes, which are symmetric with respect to m_j. Moreover, since q_2 is smooth over ∂K, we have

$$0 = \int_{\partial K} \partial_{\boldsymbol{\tau}_K} q_2 \, \mathrm{d}x = \sum_{j=1}^{3} \left|F_j\right| \partial_{\boldsymbol{\tau}_K} q_2(m_j) = \sum_{j=1}^{3} \left|F_j\right| \frac{q_2(g_j^2) - q_2(g_j^1)}{\left|F_j\right|} \sqrt{3}.$$

Hence, the following relation holds true:

$$q_2(g_1^2) - q_2(g_1^2) + q_2(g_2^2) - q_2(g_2^1) + q_2(g_3^2) - q_2(g_3^1) = 0.$$

This is a linear dependence condition involving all the degrees of freedom. Moreover, it is possible to check (Fortin & Soulie, 1983) that the quadratic polynomial $2 - 3(\lambda_1^2 + \lambda_2^2 + \lambda_3^2)$ has vanishing degrees freedom but is not zero in K. Consequently, the choice of the degrees of freedom in (14) is not suited to describe even degree CR spaces.

In order to establish a set of unisolvent degrees of freedom, the even counterpart of the explicit space in (17) comes to the rescue. With each element K in $\mathcal{T}_h$, we associate the elemental nonconforming bubble function (Stoyan & Baran, 2006)

$$b_p^K := \begin{cases} \frac{1}{2}\left(-1 + \sum_{i=1}^{3} L_p(1-2\lambda_i)\right) & \text{on } K \\ 0 & \text{otherwise.} \end{cases} \tag{22}$$

Following Stoyan & Baran (2006); Ciarlet *et al.* (2016) and Carstensen & Sauter (2022b), under the notation in Section 1.3, we define

$$V_n^{\mathrm{ex}} := \operatorname{span}\left(\varphi^v \quad \forall v \subset \mathcal{V}_h; \quad \{\varphi_j^F\}_{j=1}^{p-1} \quad \forall F \subset \mathcal{F}_h; \quad b_p^K \text{ and } \{\varphi_\ell^K\}_{\ell=1}^{(p-2)(p-1)/2} \quad \forall K \in \mathcal{T}_h\right). \tag{23}$$

As discussed in Fortin & Soulie (1983, Proposition 1) for the case $p = 2$, these functions are linearly dependent: there exists precisely one elemental nonconforming bubble that can be written as a linear combination of the other functions generating the space; some details are provided in Lemma 1.3 below.

LEMMA 1.3. The spaces V_n^{im} and V_n^{ex} defined in (13) and (23) coincide for even p.

Proof. Introduce $\Phi_n := \operatorname{span}\{b_p^K \mid K \in \mathcal{T}_h\}$. Let N_F^T, N_F^I, N_V, and N_K denote the number of total edges, internal edges, vertices, and elements of $\mathcal{T}_h$, respectively. We split the proof in two steps.

V_n^{ex} is contained in V_n^{im}. The space V_n^{ex} is defined as $X_n + \Phi_n$, i.e., it consists of modal basis functions, which are H^1 conforming and therefore contained in V_n^{im}, and elemental nonconforming bubbles as in (22). Such bubble functions have vanishing jump moments with respect to polynomials of order $p-1$ over the edges in $\mathcal{F}_h$.

To see this, we fix a generic F in $\mathcal{F}_h^I$ and one of the two elements K in ω_F. The restriction of b_p^K on F is given by the sum of four terms, see (22): two of them are (scaled) univariate Legendre polynomials of degree p, which have vanishing moments up to order $p-1$; the sum of the other two vanishes since the restriction of the remaining Legendre polynomial over F is equal to 1.

V_n^{im} and V_n^{ex} have the same dimension. As shown in the proof of Lemma 1.2, the dimension of V_n^{im} is given by

$$\dim(V_n^{\mathrm{im}}) = \dim(\mathbb{P}_p(\mathcal{T}_h)) - pN_F^I = \dim(\mathbb{P}_p(K))N_K - pN_F^I.$$

As for the dimension of V_n^{ex}, we start by investigating the dimensions of X_n and Φ_n, separately. The former is given by the number of total modal basis functions:

$$\dim(X_n) = \dim(\mathbb{P}_{p-3}(K))N_K + \dim(\mathbb{P}_{p-2}(F))N_F^T + N_V;$$

the latter by the number of elements:

$$\dim(\Phi_n) = N_K.$$

Based on the Euler's formulas (20) and $N_K - N_F^T + N_V = 1$, the dimensions of V_n^{im}, X_n, and Φ_n satisfy the following relation:

$$\dim(X_n) + \dim(\Phi_n) = \dim(V_n^{\mathrm{im}}) + 1. \tag{24}$$

As elemental bubbles of neighbouring elements have the same restriction on the interface, we have

$$X_n \cap \Phi_n = \operatorname{span}\left\{ \sum_{K \in \mathcal{T}_h} b_p^K \right\}, \qquad \dim(X_n \cap \Phi_n) = 1. \tag{25}$$

We deduce

$$\dim(V_n^{\mathrm{im}}) + 1 \overset{(24)}{=} \dim(X_n) + \dim(\Phi_n) = \dim(X_n + \Phi_n) + \dim(X_n \cap \Phi_n) \overset{(25)}{=} \dim(V_n^{\mathrm{ex}}) + 1.$$

□

Remark 3. A consequence of Lemma 1.3 is that an explicit basis for V_n^{im} and V_n^{ex} is given by the generating functions in (23), after removing one elemental nonconforming bubble; the corresponding degrees of freedom are the coefficients in the expansion with respect to that basis. Differently from the case p odd, we have not at disposal a set of degrees of freedom as those in (14). As such, it is not apparent how to derive interpolation estimates with respect to proposed type of basis. In Section 2 below, we shall propose an alternative CR construction, which allows us to circumvent this issue.

1.5 *Convergence for standard CR elements*

As we proved that the implicit and explicit CR spaces are the same, see Lemmas 1.2 and 1.3, we henceforth write V_n to denote either of the two. Moreover, given g in $L^1(\partial\Omega)$, we write

$$V_n^g := H_{p,g}^{1,nc}(\mathcal{T}_h, \Omega) \cap V_n.$$

Define the bilinear form $a_n : [H^1(\Omega) + V_n]^2 \to \mathbb{R}$ as

$$a_n(v_n, w_n) := (\nabla_h v_n, \nabla_h w_n)_{0,\Omega}. \tag{26}$$

We review (Brenner, 2015) the standard analysis of the following method:

$$\begin{cases} \text{find } u_n \in V_n^0 \text{ such that} \\ a_n(u_n, v_n) = (f, v_n)_{0,\Omega} \quad \forall v_n \in V_n^0. \end{cases} \tag{27}$$

The treatment of inhomogeneous Dirichlet boundary conditions is discussed in Section 3 below.

The bilinear form in (26) is coercive and continuous with constants 1 with respect to the broken seminorm in (5); in turn, that seminorm is a norm on V_n^0 due to (9). Therefore, method (27) is well-posed and the following convergence result holds true; its proof is standard (Brenner, 2015). We report some details as they will be needed in the analysis of new CR-type methods, see Section 2.

PROPOSITION 1.4. Let u and u_n be the solutions to (2) and (27). Then, we have

$$\left|u-u_n\right|_{1,h;\Omega} \leq \inf_{v_n\in V_n^0} \left|u-v_n\right|_{1,h;\Omega} + \sup_{v_n\in V_n^0} \frac{|a_n(u,v_n)-(f,v_n)_{0,\Omega}|}{\left|v_n\right|_{1,h;\Omega}}. \tag{28}$$

If u belongs to $H^s(\Omega)$, s larger than $3/2$, and p is smaller than or equal to s, then we have

$$\left|u-u_n\right|_{1,h;\Omega} \lesssim h^p |u|_{p+1,\Omega}. \tag{29}$$

Proof. Inequality (28) is second Strang's lemma (Strang, 1972; Brenner, 2015). As for estimate (29), we bound the two terms on the right-hand side of (28) separately.

As for the first one, the best error in CR spaces is smaller than the best error in conforming Lagrangian spaces: the convergence follows from standard polynomial interpolation theory (Brenner & Scott, 2008); the $H^s(\Omega)$ regularity, s larger than $3/2$, suffices to this purpose.

As for the second term, for all F in $\mathcal{F}_h$, introduce $\Pi_{p-1}^{0,F}$ as the orthogonal projector with respect to the $L^2(F)$ inner product into the space $\mathbb{P}_{p-1}(F)$ of polynomial vector fields. Denote the elements in ω_F by K_i, $i=1,2$. An integration by parts, definitions (6) and (7), formulation (1), the Cauchy–Schwarz inequality, and the assumption that u belongs to $H^s(\Omega)$, s larger than $3/2$, yield, for all $q_p^{K_1}$, $q_p^{K_2}$, $q_0^{K_1}$, and $q_0^{K_2}$ in $\mathbb{P}_p(K_1)$, $\mathbb{P}_p(K_2)$, $\mathbb{P}_0(K_1)$ and $\mathbb{P}_0(K_2)$,

$$\begin{aligned} a_n(u,v_n)-(f,v_n)_{0,\Omega} &= \sum_{K\in\mathcal{T}_h} (\mathbf{n}_K\cdot\nabla u, v_n)_{0,\partial K} = \sum_{F\in\mathcal{F}_h} \left(\mathbf{n}_F\cdot\nabla u, [\![v_n]\!]\right)_{0,F} \\ &= \sum_{F\in\mathcal{F}_h} \left(\mathbf{n}_F\cdot\nabla u - \Pi_{p-1}^{0,F}\mathbf{n}_F\cdot\nabla u, [\![v_n]\!] - \Pi_{p-1}^{0,F}[\![v_n]\!]\right)_{0,F}. \end{aligned} \tag{30}$$

For interior edges, we have

$$\begin{aligned} &\left(\mathbf{n}_F\cdot\nabla u - \Pi_{p-1}^{0,F}\mathbf{n}_F\cdot\nabla u, [\![v_n]\!] - \Pi_{p-1}^{0,F}[\![v_n]\!]\right)_{0,F} \\ &\leq \left\| \frac{1}{2}\mathbf{n}_{K_1}\cdot\nabla(u_{|K_1}-q_p^{K_1}) - \frac{1}{2}\mathbf{n}_{K_2}\cdot\nabla(u_{|K_2}-q_p^{K_2}) \right\|_{0,F} \left\| \frac{1}{2}(v_{n|K_1}-q_0^{K_1}) + \frac{1}{2}(v_{n|K_2}-q_0^{K_2}) \right\|_{0,F}. \end{aligned}$$

The multiplicative trace inequality, the Poincaré inequality, and choosing the polynomial vector fields above as suitable elementwise L^2 projections entail that the two terms on the right-hand side of (30) satisfy, for $i=1,2$ and positive ε,

$$\begin{aligned} \left\|\mathbf{n}_{K_i}\cdot\nabla(u_{|K_1}-q_p^{K_i})\right\|_{0,F} &\lesssim h_F^{-\frac{1}{2}} \left\|\nabla_h(u-q_p^{K_i})\right\|_{0,K_i} + h_F^{\varepsilon}\left|u-q_p^{K_i}\right|_{\frac{3}{2}+\varepsilon,K_i}; \\ \left\|v_{n|K_i}-q_0^{K_i}\right\|_{0,F} &\lesssim h_F^{-\frac{1}{2}} \left\|v_n-q_0^{K_i}\right\|_{0,K_i} + h_F^{\frac{1}{2}}|v_n|_{1,K_i} \lesssim h^{\frac{1}{2}}|v_n|_{1,K_i}. \end{aligned}$$

Analogous estimates can be proven for boundary edges. Combining the above displays with (30), and standard polynomial approximation results yield the assertion. □

REMARK 4. For odd degree p, given v in $W^{1,1}(\Omega)$, we can define v_I in V_n by fixing its degrees of freedom (14) equal to those of v. A standard Bramble-Hilbert argument entails optimal interpolation estimates under regularity assumptions that are milder than those needed for pointwise interpolation operators as used in Lemma 1.4.

REMARK 5. One of the most striking features of CR elements is that the structure of the explicit basis functions is very different in the odd and even degree cases; see (17) and (23). On the one hand, in the light of Remark 4, this renders the derivation of interpolation estimates in the p-version of the method less immediate than for conforming and DG methods. On the other hand, in the assembling process of the matrix stemming from method (27) for increasing p, it is not feasible to use the same indexing strategy for even and odd degrees since the types of basis functions under consideration change. In the odd case, modal vertex functions are not considered and edge nonconforming bubble functions are used; in the even case, modal vertex functions are considered and elemental nonconforming bubble functions are used.

2. New Crouzeix-Raviart elements of even degree

Here, we propose a different construction of even degree CR elements, which allows for circumventing some of the shortcomings discussed in Remark 5. In particular, in Section 2.1, we define a new implicit CR-type space of even degree; show an explicit construction of a corresponding spanning set of functions; identify a set of unisolvent DoFs analogous to that introduced for the standard odd case. Moreover, in Section 2.2, we propose a stabilized, arbitrary order CR-type method, which is suitable for *hp*-refinements, and prove its optimal convergence.

2.1 *Edge-bubble-type even degree Crouzeix-Raviart spaces*

Let p be an even positive integer. We define a modification of the Sobolev nonconforming space in (7) as follows:

$$\widetilde{H}^{1,nc}_p(\mathcal{T}_h,\Omega) := \left\{ \widetilde{v} \in H^1(\mathcal{T}_h,\Omega) \,\middle|\, (\llbracket \widetilde{v} \rrbracket, L^F_j)_{0,F} = 0 \quad \forall j = 0,\dots,p-2,p, \quad \forall F \in \mathcal{F}^I_h \right\}.$$

Based on this, we introduce a variant of the space V^{im}_n in (13):

$$\widetilde{V}^{\mathrm{im}}_n := \left\{ \widetilde{v}_n \in \widetilde{H}^{1,nc}_p(\mathcal{T}_h,\Omega) \,\middle|\, \widetilde{v}_{n|K} \in \mathbb{P}_p(K) \quad \forall K \in \mathcal{T}_h \right\}. \tag{31}$$

This space does not coincide with V^{im}_n: on an edge F in $\mathcal{F}_I$, the jump of $\widetilde{v}_n$ in $\widetilde{V}^{\mathrm{im}}_n$ is orthogonal with respect to polynomials in $\mathbb{P}_{p-2}(F)$ and the pth Legendre polynomial L^F_p, instead of being orthogonal with respect to $\mathbb{P}_{p-1}(F)$.

Under the notation in Section 1.4.1, we introduce a set of linear functionals similar to those in (14): on each K, given $\widetilde{v}$ in $W^{1,1}(K)$, we consider

$$|F|^{-1}(\widetilde{v}, L_j^F)_{0,F} \qquad \forall j = 0, \dots p-2, p, \quad \forall F \in \mathcal{F}^K; \tag{32a}$$

$$|K|^{-1}(\widetilde{v}, m_{\boldsymbol{\beta}}^K)_{0,K} \qquad \forall |\boldsymbol{\beta}| = 0, \dots, p-3. \tag{32b}$$

LEMMA 2.1. The linear functional (32a)-(32b) are a set of unisolvent DoFs for $\mathbb{P}_p(K)$.

Proof. The proof follows along the same lines as that of Lemma 1.1. Let $\widetilde{v}_n$ be in $\mathbb{P}_p(K)$ such that the moments (32a)–(32b) are zero. The number of linear functionals in (32a)–(32b) is equal to $\dim(\mathbb{P}_p(K))$; therefore, it suffices to prove that $\widetilde{v}_n$ is identically zero over K.

Given a edge F in $\mathcal{F}^K$, using that the edge moments (32a) vanish, we deduce that $\widetilde{v}_{n|F}$ belongs to $\mathbb{P}_p(F)$ and is orthogonal to $\operatorname{span}\{\mathbb{P}_{p-2}(F), L_p^F\}$. Hence, there exists a constant c in $\mathbb{R}$ such that $\widetilde{v}_{n|F}(\xi) = c\, L_{p-1}^F(\xi)$ for all F in $\mathcal{F}^K$. Since p is even, $L_{p-1}^F(\xi)$ is odd symmetric with respect to the midpoint of F, and $\widetilde{v}_{n|\partial K}$ belongs to $\mathcal{C}^0(\partial K)$, then the following identities are valid:

$$\widetilde{v}_n(v_1) = -\widetilde{v}_n(v_2) = \widetilde{v}_n(v_3) = -\widetilde{v}_n(v_1), \tag{33}$$

whence $\widetilde{v}_n$ is zero over ∂K. Using that the elemental moments are zero, the assertion follows as in the proof of Lemma 1.1. □

Following the construction of V_n^{ex} for odd p in (17), under the notation in Section 1.4.1, we define

$$\widetilde{V}_n^{\mathrm{ex}} := \operatorname{span}\left(b_{p-1}^F \text{ and} \{\varphi_j^F\}_{j=1}^{p-1} \quad \forall F \subset \mathcal{F}_h; \quad \{\varphi_\ell^K\}_{\ell=1}^{(p-1)(p-2)/2} \quad \forall K \in \mathcal{T}_h \right). \tag{34}$$

LEMMA 2.2. The spaces $\widetilde{V}_n^{\mathrm{im}}$ and $\widetilde{V}_n^{\mathrm{ex}}$ defined in (31) and (34) coincide for even p.

Proof. The proof is exactly the same as that of Lemma 1.2. □

Since the spaces $\widetilde{V}_n^{\mathrm{im}}$ and $\widetilde{V}_n^{\mathrm{ex}}$ coincide, we shall write $\widetilde{V}_n$ to denote either of the two; with an abuse of notation, for the odd degree case, the spaces V_n^{im} and V_n^{ex} will be henceforth denoted also by $\widetilde{V}_n^{\mathrm{im}}$ and $\widetilde{V}_n^{\mathrm{ex}}$. Given g in $L^1(\partial\Omega)$, we define $\widetilde{V}_n^g$ as $\widetilde{H}_{p,g}^{1,nc}(\mathcal{T}_h, \Omega) \cap \widetilde{V}_n$, where

$$\widetilde{H}_{p,g}^{1,nc}(\mathcal{T}_h, \Omega) := \left\{ \widetilde{v}_n \in \widetilde{H}_p^{1,nc}(\mathcal{T}_h, \Omega) \,\middle|\, (\llbracket \widetilde{v}_n \rrbracket, L_j^F)_{0,F} = (g, L_j^F)_{0,F} \quad \forall j = 0, \dots, p-2, p, \ \forall F \in \mathcal{F}_h^B \right\}. \tag{35}$$

2.2 *Optimal convergence for a stabilized CR method*

If we replace V_n in (27) by $\widetilde{V}_n$ in the case p even, then one may expect method (27) to be one order suboptimal. In fact, proceeding as in the proof of Lemma 1.4, we rewrite display (30) as follows:

$$\begin{aligned} a_n(u,\widetilde{v}_n) - (f,\widetilde{v}_n) &= \sum_{K\in\mathcal{T}_h} (\mathbf{n}_K\cdot\nabla u, \widetilde{v}_n)_{0,\partial K} = \sum_{F\in\mathcal{F}_h} (\mathbf{n}_F\cdot\nabla u, [\![\widetilde{v}_n]\!])_{0,F} \\ &= \sum_{F\in\mathcal{F}_h} \left(\mathbf{n}_F\cdot\nabla u - \Pi^{0,F}_{p-2}(\mathbf{n}_F\cdot\nabla u), [\![\widetilde{v}_n]\!] - \Pi^{0,F}_0 [\![\widetilde{v}_n]\!]\right)_{0,F}, \end{aligned}$$

which delivers an order of convergence $\mathcal{O}(h^{p-1})$ due to the presence of $\Pi^{0,F}_{p-2}$ instead of $\Pi^{0,F}_{p-1}$.

As a matter of notation, we define the operator $\Pi_{L^F_{p-1}}$ as zero if p is odd and as the $L^2(F)$ projector onto the Legendre polynomial L^F_{p-1} if p is even. In order to recover error estimates of order $\mathcal{O}(h^p)$, we modify method (27) by employing the discrete bilinear form $\widetilde{a}_n : [H^1(\Omega)+\widetilde{V}_n]^2 \to \mathbb{R}$ defined as follows: for a sufficiently large positive coefficient η, see Proposition 2.3 below,

$$\begin{aligned} \widetilde{a}_n(\widetilde{u}_n,\widetilde{v}_n) &:= (\nabla_h\widetilde{u}_n,\nabla_h\widetilde{v}_n)_{0,\Omega} - \sum_{F\in\mathcal{F}_h} \left(\Pi_{L^F_{p-1}}\mathbf{n}_F\cdot\{\nabla_h\widetilde{u}_n\}, \Pi_{L^F_{p-1}}[\![\widetilde{v}_n]\!]\right)_{0,F} \\ &- \sum_{F\in\mathcal{F}_h} \left(\Pi_{L^F_{p-1}}[\![\widetilde{u}_n]\!], \Pi_{L^F_{p-1}}\mathbf{n}_F\cdot\{\nabla_h\widetilde{v}_n\}\right)_{0,F} + \eta\sum_{F\in\mathcal{F}_h} h_F^{-1}\left(\Pi_{L^F_{p-1}}[\![\widetilde{u}_n]\!], \Pi_{L^F_{p-1}}[\![\widetilde{v}_n]\!]\right)_{0,F}. \end{aligned} \tag{36}$$

Introduce the mesh-dependent norm

$$|||\widetilde{v}_n|||_n^2 := |\widetilde{v}_n|^2_{1,h;\Omega} + \sum_{F\in\mathcal{F}_h} h_F^{-1}\left\|\Pi_{L^F_{p-1}}[\![\widetilde{v}_n]\!]\right\|^2_{0,F}. \tag{37}$$

We consider and analyze the following method:

$$\begin{cases} \text{find } \widetilde{u}_n\in\widetilde{V}^0_n \text{ such that} \\ \widetilde{a}_n(\widetilde{u}_n,\widetilde{v}_n) = (f,\widetilde{v}_n)_{0,\Omega} \qquad\qquad \forall\widetilde{v}_n\in\widetilde{V}^0_n. \end{cases} \tag{38}$$

For even p, the bilinear form $\widetilde{a}_n$ in (36) resembles that in standard symmetric interior penalty DG methods (Di Pietro & Ern, 2012), yet requires a stabilization on a one dimensional space for each edge; for odd p, the bilinear form $\widetilde{a}_n$ instead coincides with that in (26). Comments on an alternative construction for even degree CR methods are given in Remark 8 below; in particular the edge nonconforming bubbles used in (34) and the corresponding projections in (36) can be of any odd (also linear!) degree as the crucial point in the unisolvence proof is the validity of (33).

The following well-posedness and convergence result for (38) holds true.

Proposition 2.3. If η in (36) is sufficiently large, then method (38) is well-posed. Given u and $\widetilde{u}_n$ be the solutions to (2) and (38), we have

$$|||u-\widetilde{u}_n|||_n \lesssim \inf_{\widetilde{v}_n\in\widetilde{V}^0_n} |||u-\widetilde{v}_n|||_n + \sup_{\widetilde{v}_n\in\widetilde{V}^0_n} \frac{|\widetilde{a}_n(u,\widetilde{v}_n)-(f,\widetilde{v}_n)_{0,\Omega}|}{|||\widetilde{v}_n|||_n}. \tag{39}$$

If u belongs to $H^s(\Omega)$, s larger than $3/2$, and p smaller than or equal to s, we have

$$\left|\!\left|\!\left| u - \widetilde{u}_n \right|\!\right|\!\right|_n \lesssim h^p |u|_{p+1,\Omega}. \tag{40}$$

Proof. The bilinear form in (36) is coercive with respect to the mesh-dependent norm (37). Indeed, given $\widetilde{v}_n$ in $\widetilde{V}_n$, definition (36) yields

$$\widetilde{a}_n(\widetilde{v}_n, \widetilde{v}_n) = \sum_{K\in\mathcal{T}_h} |\widetilde{v}_n|^2_{1,K} - 2\sum_{F\in\mathcal{F}_h} \left(\Pi^F_{L^F_{p-1}} \mathbf{n}_F \cdot \{\nabla \widetilde{v}_n\}, \Pi_{L^F_{p-1}} [\![\widetilde{v}_n]\!] \right)_{0,F} + \eta \sum_{F\in\mathcal{F}_h} h_F^{-1} \left\| \Pi_{L^F_{p-1}} \widetilde{v}_n \right\|^2_{0,F}. \tag{41}$$

For a given K in $\mathcal{T}_h$, the following discrete trace inequality (Di Pietro & Ern, 2012, Lemma 1.46) holds true:

$$h_K^{\frac{1}{2}} \|\widetilde{v}_n\|_{0,\partial K} \lesssim \|\widetilde{v}_n\|_{0,K}. \tag{42}$$

On a fixed F in $\mathcal{F}_h$, the Cauchy–Schwarz inequality, the property $h_F \le h_K$ for K in ω_F, the stability of the L^2 projector, and the discrete trace inequality (42) yield

$$\begin{aligned}
&\sum_{F\in\mathcal{F}_h} \left(\Pi^F_{L^F_{p-1}} \mathbf{n}_F \cdot \{\nabla \widetilde{v}_n\}, \Pi_{L^F_{p-1}} [\![\widetilde{v}_n]\!] \right)_{0,F} \\
&\le \left(\sum_{F\in\mathcal{F}_h} h_F \left\| \Pi^F_{L^F_{p-1}} \mathbf{n}_F \cdot \{\nabla_h \widetilde{v}_n\} \right\|^2_{0,F} \right)^{\frac{1}{2}} \left(\sum_{F\in\mathcal{F}_h} h_F^{-1} \left\| \Pi_{L^F_{p-1}} [\![\widetilde{v}_n]\!] \right\|^2_{0,F} \right)^{\frac{1}{2}} \\
&\le \left(\sum_{K\in\mathcal{T}_h} h_K \|\nabla_h \widetilde{v}_{n|K}\|^2_{0,\partial K} \right)^{\frac{1}{2}} \left(\sum_{F\in\mathcal{F}_h} h_F^{-1} \left\| \Pi_{L^F_{p-1}} [\![\widetilde{v}_n]\!] \right\|^2_{0,F} \right)^{\frac{1}{2}} \lesssim \|\nabla_h \widetilde{v}_n\|_{0,\Omega} \left(\sum_{F\in\mathcal{F}_h} h_F^{-1} \left\| \Pi_{L^F_{p-1}} [\![\widetilde{v}_n]\!] \right\|^2_{0,F} \right)^{\frac{1}{2}}.
\end{aligned}$$

Substituting the above inequality in (41), we obtain

$$\widetilde{a}_n(\widetilde{v}_n, \widetilde{v}_n) \gtrsim \|\nabla_h \widetilde{v}_n\|^2_{0,\Omega} - \|\nabla_h \widetilde{v}_n\|_{0,\Omega} \left(\sum_{F\in\mathcal{F}_h} h_F^{-1} \left\| \Pi_{L^F_{p-1}} [\![\widetilde{v}_n]\!] \right\|^2_{0,F} \right)^{\frac{1}{2}} + \eta \sum_{F\in\mathcal{F}_h} h_F^{-1} \left\| \Pi_{L^F_{p-1}} [\![\widetilde{v}_n]\!] \right\|^2_{0,F}.$$

Further using Young's inequality, this yields the coercivity of $\widetilde{a}_n(\cdot,\cdot)$ with respect to the norm (37) for η sufficiently large. On the one hand this implies the well-posedness of method (38). On the other hand, inequality (39) follows from the second Strang's lemma (see, e.g., Strang, 1972; Brenner, 2015). The hidden constants therein depends on the discrete coercivity constant, which in turns depend on η and p.

In order to derive the error estimate (40), we show an upper bound for the two terms on the right-hand side of (39) separately. As for the first one, we observe that

$$\inf_{\widetilde{v}_n\in\widetilde{V}_n^0}\left(\sum_{K\in\mathcal{T}_h}\left\|\nabla(u-\widetilde{v}_n)\right\|_{0,K}^2+\sum_{F\in\mathcal{F}_h}h_F^{-1}\left\|\Pi_{L_{p-1}^F}\left(\left[\!\left[\widetilde{v}_n\right]\!\right]\right)\right\|_{0,F}^2\right)$$
$$\leq\inf_{\widetilde{v}_n\in\widetilde{V}_n^0}\left(\sum_{K\in\mathcal{T}_h}\left\|\nabla(u-\widetilde{v}_n)\right\|_{0,K}^2+\sum_{F\in\mathcal{F}_h}h_F^{-1}\left\|\left[\!\left[\widetilde{v}_n\right]\!\right]\right\|_{0,F}^2\right).$$

The best error in CR spaces is smaller than the error in H^1 conforming spaces; in particular the jump terms vanish. Optimal convergence follows from polynomial approximation results (Brenner & Scott, 2008).

As for the second term in (39), convergence for odd p is already discussed in Proposition 1.4. Therefore, we focus on the even p case. On all edges, $\{\nabla u\}$, $[\![u]\!]$, and $\Pi_{L_{p-1}^F}\left[\!\left[\widetilde{v}_n\right]\!\right]$ are equal to ∇u, 0, and $\left[\!\left[\widetilde{v}_n\right]\!\right]$. These identities, an integration by parts, problem (1), and the consistency of the bilinear form (36) yield

$$\begin{aligned}\widetilde{a}_n(u,\widetilde{v}_n)-(f,\widetilde{v}_n)_{0,\Omega}&=\sum_{F\in\mathcal{F}_h}\left(\mathbf{n}_F\cdot\nabla u,\left[\!\left[\widetilde{v}_n\right]\!\right]-\Pi_{p-2}^{0,F}\left[\!\left[\widetilde{v}_n\right]\!\right]\right)_{0,F}\\&\quad-\sum_{F\in\mathcal{F}_h}\left(\Pi_{L_{p-1}^F}(\mathbf{n}_F\cdot\nabla u),\Pi_{L_{p-1}^F}\left[\!\left[\widetilde{v}_n\right]\!\right]\right)_{0,F}\\&=\sum_{F\in\mathcal{F}_h}\left(\mathbf{n}_F\cdot\nabla u,\left[\!\left[\widetilde{v}_n\right]\!\right]-\Pi_{p-1}^{0,F}\left[\!\left[\widetilde{v}_n\right]\!\right]\right)_{0,F}\\&=\sum_{F\in\mathcal{F}_h}\left(\mathbf{n}_F\cdot\nabla u-\Pi_{p-1}^{0,F}(\mathbf{n}_F\cdot\nabla u),\left[\!\left[\widetilde{v}_n\right]\!\right]-\Pi_0^{0,F}\left[\!\left[\widetilde{v}_n\right]\!\right]\right)_{0,F}.\end{aligned}$$

The assertion now follows along the same lines as in the proof of Proposition 1.4. □

Remark 6. We may drop the projection operators appearing in the definition of the bilinear form in (36) and norm in (37) since the jumps of CR functions already belong to the span of a single Legendre polynomial. In fact, this is what we did in practice in the implementation of the method; see Section 3 below. An analogous comment applies to the variable order scheme detailed in Section 4 below.

3. Numerical aspects for uniform degree CR elements in 2D

Here, we are interested in assessing the numerical performance of method (38). We focus on the h- and p-versions of the method in Sections 3.1 and 3.2; since the hp-version requires additional technicalities, it will be coped with in Section 4 below. Section 3.3 is concerned with investigating the effect of the stabilization parameter on the method. Comparisons with the standard symmetric interior penalty DG and the standard CR methods are given throughout.

Test cases. We consider $\Omega := (0,1)^2$ and the exact solutions

$$u_1(x,y) = x + y \tag{43}$$

and

$$u_2(x,y) = \sin(\pi\ x)\sin(\pi\ y). \tag{44}$$

The source term and the boundary data are computed correspondingly.

Meshes. We consider sequences of shape-regular, quasi-uniform, unstructured simplicial meshes with halving diameter; in practice, these meshes are constructed using the PDE toolbox of Matlab.

Error measures. In what follows, u_n, $\widetilde{u}_n$ and u_{DG} denote the solutions to (27), (38), and a standard symmetric interior penalty DG method (Di Pietro & Ern, 2012). The practical realization of the DG method is based on the use of piecewise modal basis functions, for a fairer comparison with the other two methods; we recall for completeness the DG bilinear form

$$\begin{aligned} a_{\mathrm{DG}}(u_{\mathrm{DG}}, v_{\mathrm{DG}}) := (\nabla_h u_{\mathrm{DG}}, \nabla_h v_{\mathrm{DG}})_{0,\Omega} &- \sum_{F\in\mathcal{F}_h} \left(\mathbf{n}_F \cdot \{\nabla_h u_{\mathrm{DG}}\}, [\![v_{\mathrm{DG}}]\!]\right)_{0,F} \\ &- \sum_{F\in\mathcal{F}_h} \left([\![u_{\mathrm{DG}}]\!], \mathbf{n}_F \cdot \{\nabla_h v_{\mathrm{DG}}\}\right)_{0,F} + \eta_{\mathrm{DG}} \sum_{F\in\mathcal{F}_h} h_F^{-1} \left([\![u_{\mathrm{DG}}]\!], [\![v_{\mathrm{DG}}]\!]\right)_{0,F}, \end{aligned}$$

where η_{DG} is a sufficiently large, positive constant, which has to scale as p^2 for stability reasons.

We shall compute the following error measures:

$$E_{CR_p} := \frac{|||u - u_n|||_{\mathrm{DG}}}{|u|_{1,\Omega}}, \qquad E_{\widetilde{CR}_p} := \frac{|||u - \widetilde{u}_n|||_{\mathrm{DG}}}{|u|_{1,\Omega}}, \qquad E_{DG_p} := \frac{|||u - u_{\mathrm{DG}}|||_{\mathrm{DG}}}{|u|_{1,\Omega}}, \tag{45}$$

where the DG norm is given by

$$|||v_{\mathrm{DG}}|||_{\mathrm{DG}}^2 := |v_{\mathrm{DG}}|_{1,h;\Omega}^2 + \sum_{F\in\mathcal{F}_h} h_F^{-1} \|[\![v_{\mathrm{DG}}]\!]\|_{0,F}^2.$$

The DG norm for the new CR space coincides with the norm $|||\cdot|||_n$ in (5); the DG norm for the standard CR space is stronger than the standard norm $|\cdot|_{1,h;\Omega}$ (albeit the jump terms only involve the projection onto the scaled Legendre polynomials of order p). The reasons why we consider the full DG norm is to have a fairer comparison with the other error measures; very similar results are obtained with the broken gradient norm.

On the nestedness of the spaces $\widetilde{V}_n$ in (34). While using the new CR spaces as in (34), we employ 'essentially' hierarchical basis functions: the conforming basis functions are modal, which are hierarchical as reviewed in Section 1.3; the nonconforming bubbles are not hierarchical but are always one per edge, differently from the standard CR case. In fact, as detailed in Remark 8 below, one could actually employ 'fully' nested spaces based on using linear nonconforming bubbles. As such, it is possible to optimize the matrix assembly process.

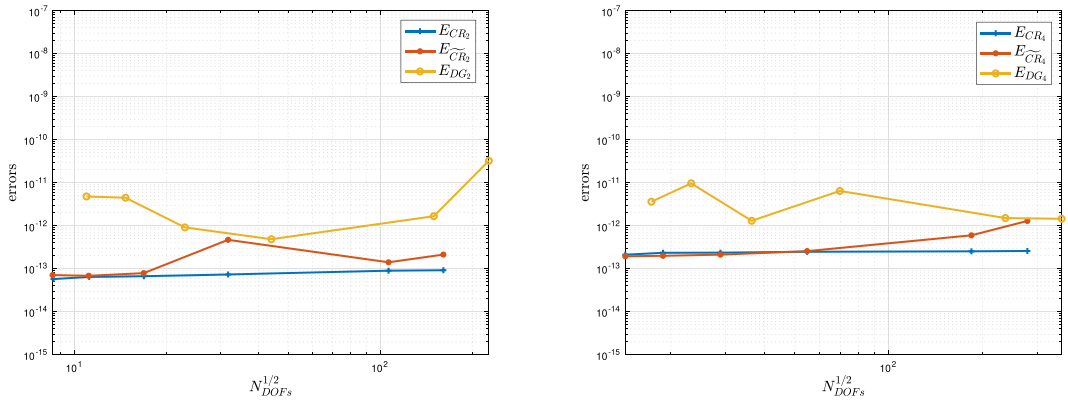

FIG. 1. Exact solution u_1 in (43); $p = 2$ and $\eta = \eta_{\mathrm{DG}} = 5$ (left panel); $p = 4$ and $\eta = \eta_{\mathrm{DG}} = 20$ (right panel). We compare the error measures in (45) under h-refinements.

Imposing Dirichlet boundary conditions. Introduce

$$\widetilde{\mathbb{P}}_p^B(\mathcal{F}_h^B) := \begin{cases} \mathbb{P}_{p-1}^B(\mathcal{F}_h^B) & \text{if } p \text{ is odd} \\ \mathrm{span}(\mathbb{P}_{p-2}(F), L_p^F \mid F \in \mathcal{F}_h^B) & \text{if } p \text{ is even.} \end{cases}$$

Possibly inhomogeneous Dirichlet boundary conditions g in $H^{\frac{1}{2}}(\partial\Omega)$ are imposed as in (35). One may alternative solve the (symmetric) mixed problem

$$\begin{cases} \text{find } \widetilde{u}_n \in \widetilde{V}_n, \widetilde{b}_n \in \widetilde{\mathcal{B}}_n := \widetilde{\mathbb{P}}_p^B(\mathcal{F}_h^B) \qquad \text{such that} \\ a_n(\widetilde{u}_n, \widetilde{v}_n) + (\widetilde{b}_n, \widetilde{v}_n)_{0,\partial\Omega} = (f, \widetilde{v}_n)_{0,\Omega} - (g, \nabla_h \widetilde{v}_n \cdot \mathbf{n}_K)_{0,\partial\Omega} \\ \qquad\qquad + \eta \sum_{F \in \mathcal{F}_h^B} h_F^{-1} (g, \widetilde{v}_n)_{0,\partial K} \qquad \forall \widetilde{v}_n \in \widetilde{V}_n \\ (\widetilde{u}_n, \widetilde{c}_n)_{0,\partial\Omega} = (g, \widetilde{c}_n)_{0,\partial\Omega} \qquad \forall \widetilde{c}_n \in \widetilde{\mathcal{B}}_n. \end{cases} \tag{46}$$

3.1 *Numerical results: h-version*

Here, we investigate the convergence of the errors in (45) under h-refinements. Since method (38) coincides with the standard CR method (27) for odd p, we consider even integers p, more precisely $p = 2$ and $p = 4$. We employ $\eta = \eta_{\mathrm{DG}} = 5$ and 20 for the two polynomial degrees.

First, we consider the exact solution u_1 in (43), which belongs to the CR and DG spaces above and is thus reproduced by all methods up to round-off errors; we display the results in Fig. 1. This test case shows how the propagation of the floating point errors depends on the number of degrees of freedom.

The errors of the two CR methods are smaller than that of the DG one. This is probably due to the fact that in the standard CR method no stabilization is employed whereas in the new one the stabilization is smaller than that for the DG one.

Next, we consider the exact solution u_2 in (44), and $\eta = 20$ for the polynomial degrees 2 and 4, and display the results in Fig. 2.

In all cases, we observe rates of convergence that are in accordance with the theoretical findings.

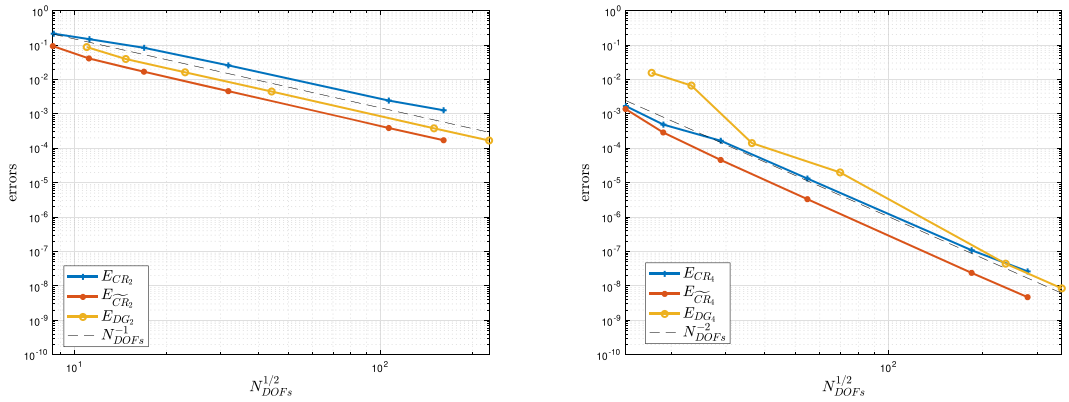

FIG. 2. Exact solution u_2 in (44); $\eta = \eta_{\mathrm{DG}} = 20$; $p = 2$ (left panel); $p = 4$ (right panel). We compare the error measures in (45) under h-refinements.

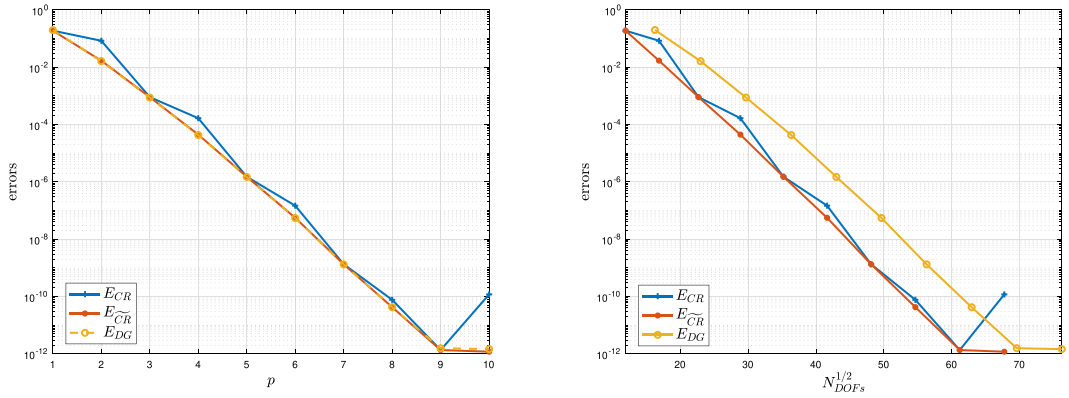

FIG. 3. Exact solution u_2 in (44); coarse fixed simplicial mesh; $\eta = \eta_{\mathrm{DG}} = 5p^2$. We compare the error measures in (45) under p-refinements with respect to the polynomial degree (left panel) and the square root of the number of degrees of freedom (right panel).

3.2 *Numerical results: p-version*

Here, we investigate the convergence of the errors in (45) under p-refinements using a fixed coarse simplicial mesh of 88 elements. We employ $\eta = \eta_{\mathrm{DG}} = 5p^2$, consider the exact solution u_2 in (44), and display the results in Fig. 3.

As expected from standard p-approximation theory, see Remark 9 below, we observe exponential convergence in terms of p.

3.3 *On the choice of the stabilization parameter*

We investigate here the performance of the errors $E_{\widetilde{CR}_p}$ and E_{DG_p} taking different values of η and η_{DG}. We consider the exact solution u_2 in (44) and compare the errors in (45) in terms of different choices of the stabilization parameters η and η_{DG}, say, in the set $\{0.5; 1; 2; 4; 8; 16; 32; 64\}$. We pick p in $\{2, 4, 6, 8\}$. We display the results in Fig. 4

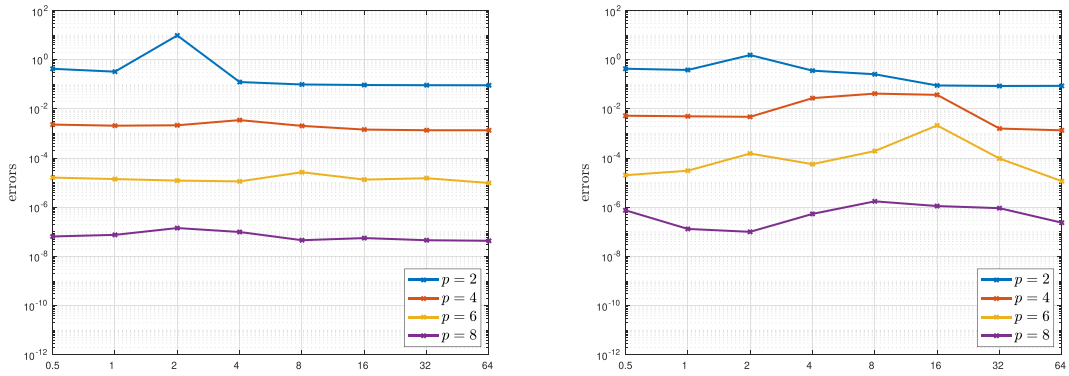

FIG. 4. Exact solution u_2 in (44); $p = 2$, 4, 6, and 8; fixed coarse simplicial mesh. We compare $E_{\widetilde{CR}_p}$ (left panel) and E_{DG_p} (right panel) picking η in $\{0.5; 1; 2; 4; 8; 16; 32; 64\}$.

It is apparent that, especially for high degree p, the errors for the DG method display a more oscillatory behaviour compared to those for the modified CR method.

4. Variable degree Crouzeix-Raviart elements

The aim of this section is to construct and analyze variable degree CR methods. After discussing why an 'obvious' construction cannot work in Section 4.1, in Section 4.2 we propose new variable order CR spaces; Section 4.3 is devoted to the design and analysis of a corresponding variable order method; in Section 4.4, we assess the performance of that method with a particular emphasis on the approximation of corner singularities under *hp*-refinements.

Notation for variable order CR spaces. For any mesh $\mathcal{T}_h$ in a given sequence, we can assume that its elements are in bijection with $\{1, 2, \ldots, \mathrm{card}(\mathcal{T}_h)\}$; let $\mathbf{p}$ be in $\mathbb{N}^{\mathrm{card}(\mathcal{T}_h)}$. With the element K (in bijection with the index j), we associate the polynomial degree $\mathbf{p}_j$ and denote it also by p_K on occasions. In what follows, with an abuse of notation, for a generic interior edge F, K_1 and K_2 denote the two elements sharing F; for a generic boundary edge F, K denotes the element such that $F = \partial K \cap \partial\Omega$.

With each edge F, we associate

$$p_F := \begin{cases} \max\{p_{K_1}, p_{K_2}\} & \text{if } F = \partial K_1 \cap \partial K_2 \\ p_K & \text{if } F = \partial K \cap \partial\Omega. \end{cases}$$

4.1 *An 'obvious' variable order CR space does not work*

We exhibit a counterexample to show why an 'obvious' construction of variable order CR spaces (and the corresponding method) cannot deliver a sequence of discrete solutions converging to the exact one.

Given p in $\mathbb{N}$, we write

$$\widetilde{p} := \begin{cases} p & \text{if } p \text{ is odd} \\ p - 1 & \text{if } p \text{ is even.} \end{cases}$$

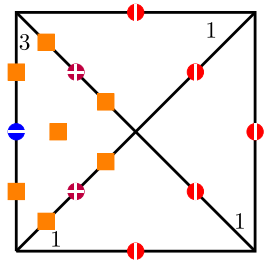

FIG. 5. Graphical representation of the degrees of freedom for an "obvious" variable order CR space over a mesh of four elements and polynomial degree distribution given by (1, 1, 1, 3). The circles (, and) stand for the coefficients of the nonconforming bubbles: in red ( ) and blue ( ), the two-sided and one-sided bubble functions of order 1 and 3 respectively; in purple ( ) the two-sided bubble functions of mixed orders 1 and 3. The squares ( ) stand for the coefficients of the modal functions. Inside each element, we write the corresponding local order.

With each internal edge F, we associate a double-sided nonconforming bubble $b^F_{\widetilde{p}_{K_1},\widetilde{p}_{K_2}}$ such that

$$b^F_{\widetilde{p}_{K_1},\widetilde{p}_{K_2}|K_j} := \begin{cases} b^F_{\widetilde{p}_{K_1}} & \text{in } K_1 \\ b^F_{\widetilde{p}_{K_2}} & \text{in } K_2 \\ 0 & \text{elsewhere,} \end{cases} \tag{47}$$

where $b^F_{\widetilde{p}_{K_1}}$ and $b^F_{\widetilde{p}_{K_2}}$ are the nonconforming bubble functions as in (16). A similar construction applies for boundary edges (only a one-sided nonconforming bubble $b^F_{\widetilde{p}_K}$ appears). As in the uniform polynomial degree case, we have $b^F_{\widetilde{p}_{K_1},\widetilde{p}_{K_2}|F} = 1$. Besides, $b^F_{\widetilde{p}_{K_1},\widetilde{p}_{K_2}}$ is nonconforming on the (four) edges of ω_F in (3).

An 'obvious' construction is as follows:

- on each element K, consider modal polynomials of order p_K excluding the (linear) hat functions;
- associate with each internal edge F shared by the elements K_1 and K_2, the double-sided nonconforming bubble function in (47);
- associate with each boundary edge F on the boundary of the element K, the one-sided nonconforming bubble function of order p_K.

An 'obvious' CR variable order space is given by the span of the functions described in the above bullets. We wish that a method associated with this space is at least first order consistent, i.e., that it reproduces affine solutions exactly up to machine precision.

Consider a mesh of four elements and a CR variable order space corresponding to polynomial degrees (1, 1, 1, 3) as detailed in Fig. 5.

In order to represent, e.g., an affine function on the left element that is nonconstant on the three edges, the coefficients of the nonconforming bubbles on that element are fixed by the three vertex values; moreover, as the involved bubbles are cubic polynomials on that element, surely all the coefficients of the cubic modal basis functions cannot vanish. Bearing this in mind, that linear function, e.g., on the bottom element, should be represented by the linear combination of the linear nonconforming bubbles (and this alone would be OK) *and* the modal basis functions where the cubic one has nonzero coefficient. This is clearly not possible, whence a cleverer construction must be in order; see Section 4.2 below. In a sense,

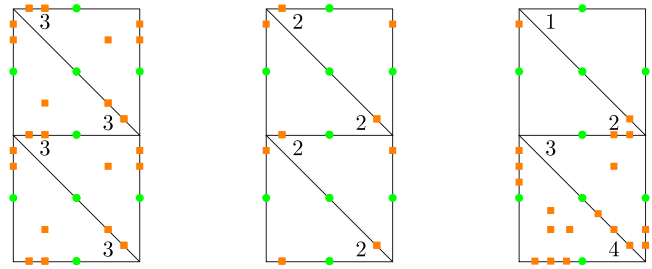

FIG. 6. Examples of global CR-type DoFs chosen as modal basis functions (■) and linear nonconforming bubbles (●) according to (48) with different degree distributions **p**.

this lack of linear consistency might be regarded as a locking property of the 'obvious' construction of variable order CR spaces as detailed above.

The main philosophy that we shall use in order to fix this issue is as follows:

- in order to avoid the locking, we shall always use linear nonconforming bubble functions (it can be readily checked on the example in Fig. 5 that in this case the modal basis functions on the edges of the left element are not active);
- since linear nonconforming bubbles have nonvanishing linear component jumps, we shall correct the method similarly to what we did in Section 1.4.2 for all orders, regardless of its parity.

4.2 *Construction of variable degree CR global spaces*

We are now in a position to exhibit an explicit version variable order CR space associated with a mesh $\mathcal{T}_h$ and a polynomial degree distribution **p**, which do not display the locking discussed in Section 4.1. Given modal basis functions as in (11) and (12), and the linear ($p = 1$) nonconforming bubble functions as in (16), we define

$$\widetilde{V}_n^{\mathrm{ex}} := \operatorname{span}\left(\widetilde{b}_1^F \text{ and } \{\varphi_j^F\}_{j=1}^{p_F-1} \quad \forall F \subset \mathcal{F}_h; \quad \{\varphi_\ell^K\}_{\ell=1}^{(p_K-1)(p_K-2)/2} \quad \forall K \in \mathcal{T}_h\right). \tag{48}$$

LEMMA 4.1. The spanning set (48) consists of linearly independent functions.

Proof. On each element, the span of the local modal basis functions is a set of linearly independent functions, which does not contain the space of continuous piecewise affine functions. That space is fixed by including also the linear nonconforming bubbles. □

A set of unisolvent degrees of freedom for the explicit space is then given by the coefficients in the expansion with respect to the basis in (48); see Fig. 6 for a graphical representation with different degree distributions **p**.

We define

$$\widetilde{H}^{1,nc}_{\mathbf{p}}(\mathcal{T}_h, \Omega) := \left\{ v_n \in H^1(\mathcal{T}_h, \Omega) \;\middle|\; \left([\![v_n]\!]_F, L_j^F \right)_{0,F} = 0 \quad \forall j = 0, \dots, p_F, j \neq 1, \forall F \in \mathcal{F}_h^I \right\}.$$

Given g in $L^1(\partial\Omega)$, we define

$$\widetilde{V}_n^{ex,g} = \widetilde{H}^{1,nc}_{\mathbf{p},g}(\mathcal{T}_h,\Omega) \cap \widetilde{V}_n^{\mathrm{ex}},$$

where

$$\widetilde{H}^{1,nc}_{\mathbf{p},g}(\mathcal{T}_h,\Omega) := \left\{ v \in \widetilde{H}^{1,nc}_{\mathbf{p}}(\mathcal{T}_h,\Omega) \,\middle|\, \left(\left[\!\left[v_n\right]\!\right], L_j^F\right)_{0,F} = \left(g, L_j^F\right)_{0,F} \quad \forall j = 0,\dots,p_F,\ j\neq 1,\ \ \forall F \in \mathcal{F}_h^B \right\}.$$

In what follows, we shall write $\widetilde{V}_n^0$ instead of $\widetilde{V}_n^{ex,g}$.

REMARK 7. $\widetilde{V}_n^{\mathrm{ex}}$ is contained in $\widetilde{H}^{1,nc}_{\mathbf{p}}(\mathcal{T}_h,\Omega)$; the proof of this fact is essentially contained in the first part of Lemmas 1.2 and 1.3.

4.3 *A variable degree CR method*

We define the operator $\Pi^{0,F}_{L_1^F}$ as the $L^2(F)$ projector onto the scaled Legendre polynomial of order 1 over F and the operator $\widetilde{\Pi}^{0,F}_{L_1^F}$ as the $L^2(F)$ projector onto the span of

$$\left\{ L_j^F \mid j = 0,\dots,p_F-1, j\neq 1 \right\}.$$

We introduce the discrete bilinear form $\widetilde{a}_n : [H^1(\Omega)+\widetilde{V}_n]^2 \to \mathbb{R}$ defined as follows: for sufficiently large positive coefficients η_F for all edges F, see Proposition 4.2 below,

$$\begin{aligned}\widetilde{a}_n(\widetilde{u}_n,\widetilde{v}_n) :=\ & (\nabla_h\widetilde{u}_n, \nabla_h\widetilde{v}_n)_{0,\Omega} - \sum_{F\in\mathcal{F}_h} \left(\Pi^{0,F}_{L_1^F} \mathbf{n}_F \cdot \{\nabla_h\widetilde{u}_n\}, \Pi^{0,F}_{L_1^F} \left[\!\left[\widetilde{v}_n\right]\!\right] \right)_{0,F} \\ & - \sum_{F\in\mathcal{F}_h} \left(\Pi^{0,F}_{L_1^F} \left[\!\left[\widetilde{u}_n\right]\!\right], \Pi^{0,F}_{L_1^F} \mathbf{n}_F \cdot \{\nabla_h\widetilde{v}_n\} \right)_{0,F} + \sum_{F\in\mathcal{F}_h} \eta_F h_F^{-1} \left(\Pi^{0,F}_{L_1^F} \left[\!\left[\widetilde{u}_n\right]\!\right], \Pi^{0,F}_{L_1^F} \left[\!\left[\widetilde{v}_n\right]\!\right] \right)_{0,F}. \end{aligned} \tag{49}$$

Introduce the mesh-dependent norm, for which Remark 6 still applies,

$$\left|\!\left|\!\left| \widetilde{v}_n \right|\!\right|\!\right|_n^2 := \sum_{K\in\mathcal{T}_h} \left\| \nabla\widetilde{v}_n \right\|_{0,K}^2 + \sum_{F\in\mathcal{F}_h} h_F^{-1} \left\| \Pi^{0,F}_{L_1^F} \left[\!\left[\widetilde{v}_n\right]\!\right] \right\|_{0,F}^2. \tag{50}$$

We consider and analyze the following method:

$$\begin{cases} \text{find } \widetilde{u}_n \in \widetilde{V}_n^0 \text{ such that} \\ \widetilde{a}_n(\widetilde{u}_n,\widetilde{v}_n) = (f,\widetilde{v}_n)_{0,\Omega} \qquad\qquad \forall \widetilde{v}_n \in \widetilde{V}_n^0. \end{cases} \tag{51}$$

The following well-posedness and convergence result for method (51) holds true.

PROPOSITION 4.2. If η_F is sufficiently large for all F in $\mathcal{F}_h$, then method (51) is well-posed. Given u and $\widetilde{u}_n$ be the solutions to (2) and (51), we have

$$\left|\!\left|\!\left| u - \widetilde{u}_n \right|\!\right|\!\right|_n \lesssim \inf_{\widetilde{v}_n \in \widetilde{V}_n^0} \left|\!\left|\!\left| u - \widetilde{v}_n \right|\!\right|\!\right|_n + \sup_{\widetilde{v}_n \in \widetilde{V}_n^0} \frac{|\widetilde{a}_n(u, \widetilde{v}_n) - (f, \widetilde{v}_n)_{0,\Omega}|}{\left|\!\left|\!\left| \widetilde{v}_n \right|\!\right|\!\right|_n}. \tag{52}$$

If u belongs to $H^s(\Omega)$, s larger than $3/2$, and p_K smaller than or equal to s for all K in $\mathcal{T}_h$, we have

$$\left|\!\left|\!\left| u - \widetilde{u}_n \right|\!\right|\!\right|_n^2 \lesssim \sum_{K \in \mathcal{T}_h} (h_K^{p_K})^2 |u|_{p_K+1,K}^2. \tag{53}$$

Proof. The bilinear form in (49) is coercive with respect to the mesh-dependent norm (50). Similarly to what we did in the proof of Proposition 2.3, this fact is a consequence of arguments that are standard in variable order symmetric interior penalty DG methods; we refer to Di Pietro & Ern (2012, Lemma 4.12). On the one hand this implies the well-posedness of method (51) for sufficiently large η_F for all F in $\mathcal{F}_h$.

On the other hand, inequality (52) follows from the second Strang's lemma (see, e.g., Strang, 1972; Brenner, 2015). The hidden constants therein depends on the discrete coercivity constant, which in turns depends on the collection of the stabilization parameters η_F and the polynomial degree distribution $\mathbf{p}$.

In order to derive estimate (53), we show an upper bound for the two terms on the right-hand side of (52) separately. As for the first one, we observe that

$$\begin{aligned}
&\inf_{\widetilde{v}_n \in \widetilde{V}_n^0} \left(\sum_{K \in \mathcal{T}_h} \left\| \nabla (u - \widetilde{v}_n) \right\|_{0,K}^2 + \sum_{F \in \mathcal{F}_h} h_F^{-1} \left\| \Pi_{L_1^F}^{0,F} [\![\widetilde{v}_n]\!] \right\|_{0,F}^2 \right) \\
&\lesssim \inf_{\widetilde{v}_n \in \widetilde{V}_n^0} \left(\sum_{K \in \mathcal{T}_h} \left\| \nabla (u - \widetilde{v}_n) \right\|_{0,K}^2 + \sum_{F \in \mathcal{F}_h} h_F^{-1} \left\| [\![\widetilde{v}_n]\!] \right\|_{0,F}^2 \right).
\end{aligned}$$

The best error in CR spaces is smaller than the error in H^1 conforming spaces; in particular the jump terms vanish. Optimal convergence follows from polynomial approximation results (Schwab, 1998).

As for the second term in (52), we observe that $\{\nabla u\}$, $[\![u]\!]$, and $\Pi_{L_1^F}^{0,F} [\![\widetilde{v}_n]\!]$ are equal to ∇u, 0, and $[\![\widetilde{v}_n]\!]$, respectively, on all edges. These identities, an integration by parts, problem (1), and the consistency of the bilinear form (49) yield

$$\begin{aligned}
\widetilde{a}_n(u, \widetilde{v}_n) - (f, \widetilde{v}_n)_{0,\Omega} &= \sum_{F \in \mathcal{F}_h} \left(\mathbf{n}_F \cdot \nabla u, [\![\widetilde{v}_n]\!] - \widetilde{\Pi}_{L_1^F}^{0,F} [\![\widetilde{v}_n]\!] \right)_{0,F} - \sum_{F \in \mathcal{F}_h} \left(\Pi_{L_1^F}^{0,F} (\mathbf{n}_F \cdot \nabla u), \Pi_{L_1^F}^{0,F} [\![\widetilde{v}_n]\!] \right)_{0,F} \\
&= \sum_{F \in \mathcal{F}_h} \left(\mathbf{n}_F \cdot \nabla u, [\![\widetilde{v}_n]\!] - \Pi_{p_F-1}^{0,F} [\![\widetilde{v}_n]\!] \right)_{0,F} = \sum_{F \in \mathcal{F}_h} \left(\mathbf{n}_F \cdot \nabla u - \Pi_{p_F-1}^{0,F} (\mathbf{n}_F \cdot \nabla u), [\![\widetilde{v}_n]\!] - \Pi_0^{0,F} [\![\widetilde{v}_n]\!] \right)_{0,F}.
\end{aligned}$$

The assertion now follows along the same line as in the proof of Proposition 1.4. □

REMARK 8. A low hanging fruit of the proofs of Lemma 4.1 and Proposition 4.2 is that the construction of fixed even degree CR elements as in Section 2 can be easily replaced by using spaces of modal functions

as above and *linear* (or also cubic, quintic, ... instead of order $p-1$) nonconforming bubble functions; the corresponding method should contain correction terms acting on the edge projection onto a single scaled linear (or cubic, quintic, ...) Legendre polynomial. Of course, one may also wish to construct odd degree CR elements based on using linear nonconforming bubbles. In this case, the correction term, which is needed to recover convergence of order p and not for well-posedness reasons, should be included in the method as well for it to work. The price to pay would be the presence of a stabilization term; the upside would be the availability of nested bases in a p-refinement procedure.

REMARK 9. In the proof of the error estimates (53), one may also keep track of the explicit dependence on the polynomial degree distribution $\mathbf{p}$. In particular, one may derive

- algebraic convergence for uniformly increasing p and singular solutions;
- exponential convergence with respect to uniformly increasing p for analytic solutions;
- exponential convergence with respect to the cubic root of the number of degrees of freedom for solutions with corner singularities, using sequences of meshes that are geometrically refined towards the corners of the domain, and distributions of polynomial degrees that are linearly increasing with the distance from the corners.

While we postpone the discussion of a practical investigation of this aspect to Section 4.4 below, we refer to Babuška & Suri (1987) and Schwab (1998) for the appropriate *hp*-approximation and convergence results.

4.4 *Numerical investigation of the hp-version of the CR method*

Here, we assess the numerical performance of method (51) for the approximation of corner singularities using *hp*-refinements.

Test case. We consider the L-shaped domain $\Omega := (-1,1)^2 \backslash [(0,1) \times (-1,0)]$ and the exact solution

$$u_3(r,\theta) = r^{\frac{2}{3}} \sin\left(\frac{2}{3}\theta\right). \tag{54}$$

The source term and the boundary data are computed accordingly.

Meshes and polynomial degree distributions. We consider sequences of shape-regular locally quasi-uniform simplicial meshes $\{\mathcal{T}_n\}$ obtained via geometric refinements at the re-entrant corner of the L-shaped domain; the first three elements in the sequence are depicted in Fig. 7, where the geometric grading factor is $1/2$. In particular, the decomposition of each mesh $\mathcal{T}_n$ consists of $n+1$ layers defined recursively as follows: $\mathcal{L}^0$ is the set of elements abutting $(0,0)$;

$$\mathcal{L}^i := \left\{ K_1 \in \mathcal{T}_n \,|\, \overline{K_1} \cap \overline{K_2} \neq \emptyset,\ K_2 \in \mathcal{L}^{i-1},\ K_1 \notin \cup_{k=0}^{i-1} \mathcal{L}^k \right\} \qquad i = 1, \ldots, n.$$

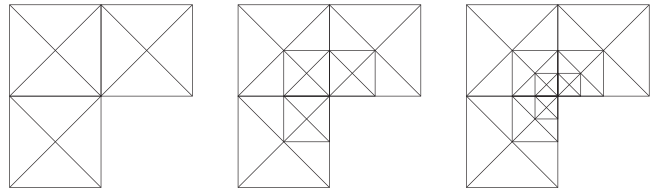

FIG. 7. First three elements in a sequence of geometrically graded meshes (with grading parameter 1/2) towards the re-entrant corner: $\mathcal{T}_0$ (left panel), $\mathcal{T}_1$ (centre panel), $\mathcal{T}_2$ (right panel).

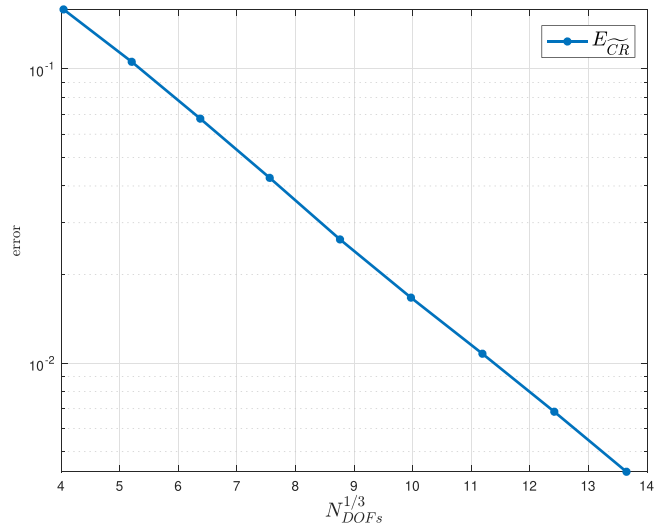

FIG. 8. Exact solution u_3 in (54); we consider a sequence of geometrically graded meshes (with grading parameter 1/2) towards the re-entrant corner as in Fig. 7, and linearly increasing polynomial degree distributions as in (55). We plot the CR error in (45) versus the cubic root of the number of degrees of freedom.

In order to obtain $\mathcal{T}_{n+1}$ from $\mathcal{T}_n$, exclusively the elements belonging to the layer $\mathcal{L}^0$ are refined. As for the polynomial distribution $\mathbf{p}$, we set

$$p_K = i + 1 \qquad \text{for all } K \text{ in } \mathcal{L}^i, \qquad i = 0, \ldots, \text{n}. \tag{55}$$

Numerical results. In Fig. 8, we display the results.

Exponential convergence as discussed in Remark 9 is observed. A similar convergence is observed, and not reported, for the L^2 error.

5. New Crouzeix-Raviart elements of even degree for the Stokes' equations

Crouzeix-Raviart elements were introduced (Crouzeix & Raviart, 1973) as an inf-sup stable, balanced, and elementwise divergence free pair for the discretization of the Stokes' equations. Even though the

main focus of this work is on second order elliptic problems, we are interested in designing new even degree CR-type elements and their practical stability.

For a given $\mathbf{f}$ in $[L^2(\Omega)]^2$, consider the Stokes' problem

$$\begin{cases} \text{find } (\mathbf{u}, s) \text{ such that} & \\ -\boldsymbol{\Delta}\mathbf{u} - \nabla s = \mathbf{f} & \text{in } \Omega \\ \operatorname{div} \mathbf{u} = 0 & \text{in } \Omega \\ \mathbf{u} = \mathbf{0} & \text{on } \partial\Omega. \end{cases} \tag{56}$$

A weak formulation of (56) reads as follows:

$$\begin{cases} \text{find } (\mathbf{u}, s) \in [H^1_0(\Omega)]^2 \times L^2_0(\Omega) =: \mathbf{V} \times Q \text{ such that} & \\ (\nabla\mathbf{u}, \nabla\mathbf{v})_{0,\Omega} + (\operatorname{div}\mathbf{v}, s)_{0,\Omega} = (\mathbf{f}, \mathbf{v})_{0,\Omega} & \forall \mathbf{v} \in \mathbf{V} \\ (\operatorname{div}\mathbf{u}, q)_{0,\Omega} = 0 & \forall q \in Q. \end{cases} \tag{57}$$

The well-posedness and analysis of this problem is standard Boffi *et al.* (2013).

We consider vector-valued CR-type spaces $\widetilde{\mathbf{V}}_n$ of order p, see Section 2.1, and piecewise polynomials $\mathbb{P}_{p-1}(\mathcal{T}_h) := \widetilde{Q}_n$ of order $p-1$ as approximation spaces to $\mathbf{V}$ and Q, respectively; let $\widetilde{\mathcal{B}}_n$ be the vector version of the corresponding space as in (46). We consider the following method, which already incorporates the imposition of the Dirichlet boundary condition for the velocity and the zero average condition for the pressure as Lagrange multipliers:

$$\begin{cases} \text{find } (\widetilde{\mathbf{u}}_n, \widetilde{\mathbf{b}}_n, \widetilde{s}_n, \widetilde{\lambda}_n) \in \widetilde{\mathbf{V}}_n \times \widetilde{\mathcal{B}}_n \times \widetilde{Q}_n \times \mathbb{R} \text{ such that} & \\ \widetilde{a}_n(\widetilde{\mathbf{u}}_n, \widetilde{\mathbf{v}}_n)_{0,\Omega} + (\widetilde{\mathbf{b}}_n, \widetilde{\mathbf{v}}_n)_{0,\partial\Omega} + (\widetilde{s}_n, \operatorname{div}_h \widetilde{\mathbf{v}}_n)_{0,\Omega} = (\mathbf{f}, \widetilde{\mathbf{v}}_n)_{0,\Omega} & \forall \widetilde{\mathbf{v}}_n \in \widetilde{\mathbf{V}}_n \\ (\widetilde{\mathbf{u}}_n, \widetilde{\mathbf{c}}_n)_{0,\partial\Omega} = 0 & \forall \widetilde{\mathbf{c}}_n \in \widetilde{\mathcal{B}}_n \\ (\operatorname{div}_h \widetilde{\mathbf{u}}_n, \widetilde{q}_n)_{0,\Omega} + (\widetilde{\lambda}_n, \widetilde{q}_n)_{0,\Omega} = 0 & \forall \widetilde{q}_n \in \widetilde{Q}_n \\ (\widetilde{s}_n, \widetilde{\mu}_n)_{0,\Omega} = 0 & \forall \widetilde{\mu}_n \in \mathbb{R}. \end{cases} \tag{58}$$

This method coincides with the standard CR method if p is odd, whereas for even p it employs the novel CR-type space as discussed in Section 2.1.

In matrix form, method (58) reads as follows (with obvious notation):

$$\begin{pmatrix} \mathbf{A}_n & \mathbf{C}_n^* & \mathbf{B}_n^* & \mathbf{0} \\ \mathbf{C}_n & \mathbf{0} & \mathbf{0} & \mathbf{0} \\ \mathbf{B}_n & \mathbf{0} & \mathbf{0} & \mathbf{D}_n^* \\ \mathbf{0} & \mathbf{0} & \mathbf{D}_n & 0 \end{pmatrix} \begin{pmatrix} \mathbf{u}_n \\ \mathbf{b}_n \\ \mathbf{s}_n \\ \lambda_n \end{pmatrix} = \begin{pmatrix} \mathbf{f}_n \\ \mathbf{0} \\ \mathbf{0} \\ 0 \end{pmatrix}.$$

5.1 *Numerical results: Stokes' equations*

Here, we investigate the convergence of method (58) on the numerical level.

Error measures. In what follows, $(\mathbf{u}_n, s)$ and $(\widetilde{\mathbf{u}}_n, \widetilde{s}_n)$ denote the solutions to (57) and (58). We shall compute the following error measures:

$$E^{Q}_{\widetilde{CR}_p} := \frac{\|s - \widetilde{s}_n\|_{0,\Omega}}{\|s\|_{0,\Omega}}, \qquad E^{V}_{\widetilde{CR}_p} := \frac{|||\mathbf{u} - \widetilde{\mathbf{u}}_n|||_n}{|\mathbf{u}|_{1,\Omega}}, \tag{59}$$

where $|||\cdot|||_n$ is the vector-valued version of that defined in (37).

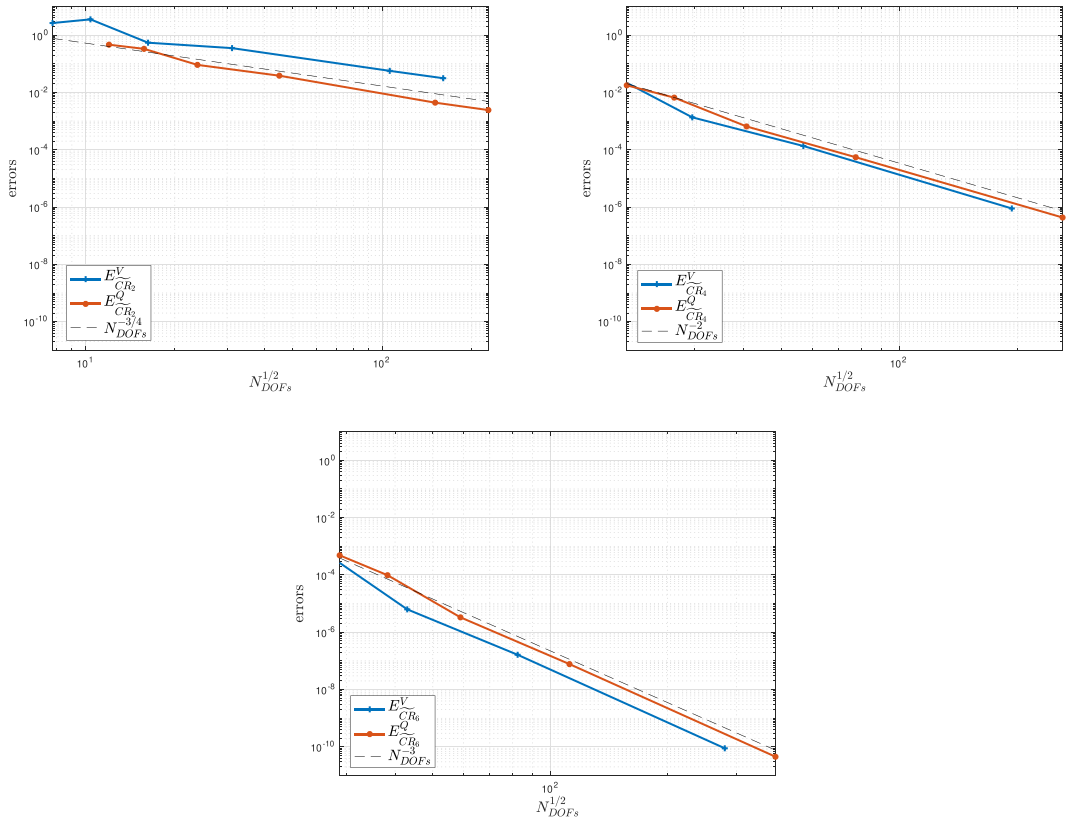

FIG. 9. Exact solution $\mathbf{u}_4$ and s_4 in (60); $p = 2$ (top-left panel); $p = 4$ (top-right panel); $p = 6$ (bottom panel); $n = 20$. We display the error measures in (59) under -refinements.

Test case. We consider the polynomial degrees $p = 4$ and 6, and the manufactured solution $\mathbf{u}_4 = [(\mathbf{u}_4)_1; (\mathbf{u}_4)_2]$ and s_4 given by

$$\begin{aligned}(\mathbf{u}_4)_1(x,y) &= -\cos\left(\pi\left(x-\frac{1}{2}\right)\right)^2 \cos\left(\pi\left(y-\frac{1}{2}\right)\right)^2 \sin\left(\pi\left(y-\frac{1}{2}\right)\right)^2;\\ (\mathbf{u}_4)_2(x,y) &= \cos\left(\pi\left(x-\frac{1}{2}\right)\right)^2 \cos\left(\pi\left(y-\frac{1}{2}\right)\right)^2 \sin\left(\pi\left(x-\frac{1}{2}\right)\right)^2;\\ s_4(x,y) &= x+y-1,\end{aligned} \tag{60}$$

on the unit square $\Omega := (0,1)^2$; the loading term and boundary conditions are computed accordingly. We consider the same sequence of meshes employed in Section 3.1.

Numerical results. In Fig. 9, we display the results.

We observe convergence of orders 4 and 6 for the methods of corresponding order; as such, the method is inf-sup stable; similar results are obtained for higher orders but are not reported here. On the other hand, we observe half an order suboptimal convergence for the case $p = 2$; this and standard

well-posedness results for mixed problems suggest that the inf-sup constant in this case is not robust with respect to the mesh size and may be behaving like $\mathcal{O}(h^{\frac{1}{2}})$.

We could have partially expected all these facts. In fact, the proposed discrete pairs lie in between the Scott-Vogelius ones (Scott & Vogelius, 1985) (which are stable for p larger than or equal to 4, and meshes without singular vertices) and that given by discontinuous velocities and pressures (Baker *et al.*, 1990): the method for even degree larger than 2 must be inf-sup stable; on the other hand, nothing could have been expected a priori for the quadratic case, since also the Scott-Vogelius element is not stable.

6. Conclusions

We constructed new CR elements and corresponding methods of even degree p for a two dimensional Poisson problem: such spaces are the span of modal functions excluding those associated with the vertices of the given mesh and edge nonconforming bubble functions of a suitable odd degree thus mimicking what happens in the odd degree CR spaces; the method required a DG-type stabilization in order to deliver convergence rates of order p.

The reason for introducing such spaces was twofold:

- for increasing polynomial order, we wanted to construct sequences of spaces spanned by functions with a 'hierarchical' structure (or even nested bases);
- we wanted to establish the ground for a simple and optimal design of variable order CR elements.

The heart of the matter in the novel construction is the observation that adding even degree nonconforming bubble functions to the modal basis yields a set of linearly dependent functions. This is not the case while using odd degree nonconforming bubbles, the intrinsic reason being described in displays (15) and (21). The price to pay is the need of stabilizing the method in order not to lose convergence.

Variable order CR elements were designed; employing *hp*-refinements yielded exponential convergence in terms of the cubic root of the degrees of freedom for solutions displaying a singular behaviour at the corners of the physical domain. Importantly,

- for the construction of fixed even degree p CR elements, nonconforming bubbles of odd degree 1 (or 3, 5, ...) can be employed;
- for the design of variable order CR elements, we use linear nonconforming bubbles so as to retain the linear consistency of the method; for this reason, we also had to stabilize the method on the edges of local odd degree larger than 1.

We further investigated whether the novel approach could fit in an inf-sup stable discretization of the Stokes' equations, which preserves the elementwise incompressibility constraint on the discrete level. This was in fact the case for even polynomial degrees larger than 2; for the quadratic element, we observed lack of inf-sup stability, which resembles that for the quadratic Scott-Vogelius element.

Acknowledgements

The authors are grateful to the anonymous referees whose comments allowed us to improve a previous version of the manuscript. The authors are also members of GNCS-INDAM.

Funding

Italian Ministry of University and Research (MUR) (PRIN2022 research grant n. 2022A79M75 to A.B.); partially funded by MUR (PRIN2022 research grant n. 202292JW3F to L.M. and M.M.) and partially funded by the European Union (ERC, NEMESIS, project number 101115663 to L.M.). Views and opinions expressed are however those of the authors only and do not necessarily reflect those of the EU or the ERC Executive Agency.

References

Ainsworth, M. & Rankin, R. (2008) Fully computable bounds for the error in nonconforming finite element approximations of arbitrary order on triangular elements. *SIAM J. Numer. Anal.*, **46**, 3207–3232.

Ayuso de Dios, B., Lipnikov, K. & Manzini, G. (2016) The nonconforming virtual element method. *ESAIM Math. Model. Numer. Anal.*, **50**, 879–904.

Babuška, I. & Suri, M. (1987) The *h-p* version of the finite element method with quasi-uniform meshes. *RAIRO Modél. Math. Anal. Numér.*, **21**, 199–238.

Baker, G. A., Jureidini, W. N. & Karakashian, O. A. (1990) Piecewise solenoidal vector fields and the Stokes problem. *SIAM J. Numer. Anal.*, **27**, 1466–1485.

Baran, Á. & Stoyan, G. (2007) Gauss-Legendre elements: a stable, higher order non-conforming finite element family. *Computing*, **79**, 1–21.

Beirão da Veiga, L., Brezzi, F., Marini, L. D. & Russo, A. (2023) The virtual element method. *Acta Numer.*, **32**, 123–202.

Boffi, D., Brezzi, F. & Fortin, M. (2013) *Mixed Finite Element Methods and Applications*, Springer Series in Computational Mathematics, vol. **44**. Heidelberg: Springer.

Brenner, S. C. (2003) Poincaré-Friedrichs inequalities for piecewise H^1 functions. *SIAM J. Numer. Anal.*, **41**, 306–324.

Brenner, S. C. (2015) Forty years of the Crouzeix-Raviart element. *Numer. Methods Partial Diff. Equ.*, **31**, 367–396.

Brenner, S. C. & Scott, L. R. (2008) *The Mathematical Theory of Finite Element Methods*, Texts in Applied Mathematics, vol. **15**, 3rd edn. New York: Springer.

Brezzi, F. & Marini, L. D. (2021) Finite elements and virtual elements on classical meshes. *Vietnam J. Math.*, **49**, 871–899.

Carstensen, C. & Sauter, S. A. (2022a) Critical functions and inf-sup stability of Crouzeix-Raviart elements. *Comput. Math. Appl.*, **108**, 12–23.

Carstensen, C. & Sauter, S. A. (2022b) Crouzeix-Raviart triangular elements are inf-sup stable. *Math. Comp.*, **91**, 2041–2057.

Cha, Y., Lee, M. & Lee, S. (2000) Stable nonconforming methods for the Stokes problem. *Appl. Math. Comput.*, **114**, 155–174.

Ciarlet, P. G., Ciarlet, P., Sauter, S. A. & Simian, C. (2016) Intrinsic finite element methods for the computation of fluxes for Poisson's equation. *Numer. Math.*, **132**, 433–462.

Crouzeix, M. & Falk, R. S. (1989) Nonconforming finite elements for the Stokes problem. *Math. Comp.*, **52**, 437–456.

Crouzeix, M. & Raviart, P.-A. (1973) Conforming and nonconforming finite element methods for solving the stationary Stokes equations. *I. Rev. Française Automat. Informat. Recherche Opérationnelle Sér. Rouge*, **7**, 33–75.

Di Pietro, D. A. & Ern, A. (2012) *Mathematical Aspects of Discontinuous Galerkin Methods*, Mathématiques & Applications, vol. **69**. Heidelberg: Springer.

Di Pietro, D. A., Ern, A. & Lemaire, S. (2014) An arbitrary-order and compact-stencil discretization of diffusion on general meshes based on local reconstruction operators. *Comput. Methods Appl. Math.*, **14**, 461–472.

Di Pietro, D. A., Ern, A. & Lemaire, S. (2016) A review of hybrid high-order methods: formulations, computational

aspects, comparison with other methods. *Building bridges: connections and challenges in modern approaches to numerical partial differential equations*, vol. **114** of Lecture Notes in Computational Science and Engineering, Cham: Springer, 205–236.

Ern, A. & Guermond, J.-L. (2021) *Finite Elements I—Approximation and Interpolation*, Texts in Applied Mathematics, vol. **72**. Cham: Springer.

Fortin, M. & Soulie, M. (1983) A nonconforming piecewise quadratic finite element on triangles. *Internat. J. Numer. Methods Engrg.*, **19**, 505–520.

Meyers, N. G. & Serrin, J. (1964) *H=W. Proc. Nat. Acad. Sci. U.S.A.*, **51**, 1055–1056.

Raviart, P.-A. & Thomas, J. M. (1977) Primal hybrid finite element methods for 2nd order elliptic equations. *Math. Comp.*, **31**, 391–413.

Sauter, S. (2023) The inf-sup constant for *hp*-Crouzeix-Raviart triangular elements. *Comput. Math. Appl.*, **149**, 49–70.

Sauter, S. & Torres, C. (2023) On the inf-sup stability of Crouzeix-Raviart Stokes elements in 3D. *Math. Comp.*, **92**, 1033–1059.

Schwab, C. (1998) *p- and hp-Finite Element Methods: Theory and Applications in Solid and Fluid Mechanics*. The Clarendon Press, Oxford University Press.

Scott, L. R. & Vogelius, M. (1985) Norm estimates for a maximal right inverse of the divergence operator in spaces of piecewise polynomials. *ESAIM Math. Model. Numer. Anal.*, **19**, 111–143.

Shen, J., Tang, T. & Wang, L.-L. (2011) *Spectral Methods: Algorithms, Analysis and Applications,* Springer Series in Computational Mathematics, vol. **41**. Heidelberg: Springer.

Stoyan, G. & Baran, Á. (2006) Crouzeix-Velte decompositions for higher-order finite elements. *Comput. Math. Appl.*, **51**, 967–986.

Strang, G. (1972) Variational Crimes in the Finite Element Method. *The Mathematical Foundations of the Finite Element Method with Applications to Partial Differential Equations (Proc. Sympos., Univ. Maryland, Baltimore, Md., 1972)*. New York-London: Academic Press, 689–710.

Szabó, B. & Babuška, I. (1991) *Finite Element Analysis*. A Wiley-Interscience Publication. New York: John Wiley & Sons, Inc.